DESIGN, ANALYSIS AND DEVELOPMENT OF A QUADRUPED ROBOT

A Final Year Project Report

Presented to

SCHOOL OF MECHANICAL & MANUFACTURING ENGINEERING

Department of Mechanical Engineering

NUST

ISLAMABAD, PAKISTAN

In Partial Fulfillment
of the Requirements for the Degree of
Bachelor of Mechanical Engineering

by

Muhammad Emaaz Azeem Jaffry
Ibrahim Bin Ali Khan
Irteza Ali Ahmed Faruqi
Haseeb Altaf Qasim

June 2022

EXAMINATION COMMITTEE

We hereby recommend that the final year project report prepared under our supervision by:

MUHAMMAD EMAAZ AZEEM JAFFRY	00000241647
IBRAHIM BIN ALI KHAN	00000251464
IRTEZA ALI AHMED FARUQI	00000241836
HASEEB ALTAF QASIM	00000246120

Titled: "DESIGN, ANALYSIS AND DEVELOPMENT OF A QUADRUPED ROBOT" be accepted in partial fulfillment of the requirements for the award of BACHELOR OF MECHANICAL ENGINEERING degree with grade ___

Supervisor: Sara Baber, Dr. (Associate Professor) Dept. of RIME, SMME	Dated:
Committee Member: Yasar Ayaz, Dr. (Professor) Dept. of RIME, SMME	Dated:
Committee Member: Khawaja Fahad, Dr. (Asst. Professor) Dept. of RIME, SMME	Dated:

_____ _____

(Head of Department) (Date)

COUNTERSIGNED

Dated: _____ _____

(Dean / Principal)

ABSTRACT

Mobile robotics comprises a wide variety of locomotion, from drones to wheeled robots and even multi-legged robots that mimic the nature around us. There have been vast amounts of research and development in the drones and wheeled robot domains. However, the relatively unexplored field of legged locomotion has greater such potential. Legged robots represent a class of ground robots that make use of articulated linkages and specific control systems to move about. Compared to wheeled robots, legged robots can exploit discontinuous pathways and isolated footholds with great efficiency, thereby increasing their reach ability. Legged locomotion is fundamentally periodic in nature with well-defined flight and stance phases in each gait cycle; this cyclic nature is exploited to increase energy efficiency in all legged creatures. These gaits can be utilized differently with respect to the terrain that is explored.

In this report, a quadruped robot based on the gait of quadruped mammals is presented by utilizing an elastically loaded scissors mechanism. This allows for a relatively smaller diameter pulley to be used, as instead of pulling on the distal joint, a proximal joint is now created, by the addition of a link, that can be used to retract the entire leg with a smaller angular displacement of the pulley. The smaller input angles required provide a greater mechanical advantage relative to the SLP mechanism. The ability of the leg to be retracted through the proximal joint faster allows for a greater stepping frequency, which in turn increases the speed of the quadruped. A robust mechanical assembly is designed and structurally improved for reduced mass and inertia. The system is tested with several motor placements in the design phase and their performance has been evaluated and their merits and demerits are gauged. The actuators are chosen based on torque calculations. After several iterations, the mechanical design is finalized. Further experiments may be conducted to further study the legged mechanism for different gaits on a planar test bed for planar walking and running motion in addition to the effects of the underlying dynamics dictated by leg for static and dynamic stability. In addition, different gaits will be applied using control system.

ACKNOWLEDGMENTS

We would like to make our acknowledgements to Dr. Sara Baber who has provided valuable and critical feedback throughout the elapsed duration of this project. Her unflinching and straightforward remarks have enabled us to capitalize on our strengths and improve our weaknesses to maximize productivity. We would also like to thank Dr. Yasar Ayaz who has given us continuous support throughout the project and has endured our frequent visits for ideas and feedback. Lastly, we appreciate the help rendered to us by Dr. Khawaja Fahad in selecting the appropriate material for the prototype development.

ORIGINALITY REPORT

ORIGINALITY REPORT

15%	%	15%	%
SIMILARITY INDEX	INTERNET SOURCES	PUBLICATIONS	STUDENT PAPERS

PRIMARY SOURCES

1	Muhammad Hamza Asif Nizami, Zaid Ahsan Shah, Yasar Ayaz, Muhammad Jawad Khan et al. "Proximal Actuation of an Elastically Loaded Scissors Mechanism for the Leg Design of a Quadruped Robot", IEEE Access, 2020 Publication	4%
2	Hamza Asif, Zaid Ahsan Shah, Yasar Ayaz, Muhammad Jawad Khan et al. "Proximal Actuation of an Elastically Loaded Scissors Mechanism for the Leg Design of a Quadruped Robot", IEEE Access, 2020 Publication	3%
3	Nathan Kau, Aaron Schultz, Natalie Ferrante, Patrick Slade. "Stanford Doggo: An Open-Source, Quasi-Direct-Drive Quadruped", 2019 International Conference on Robotics and Automation (ICRA), 2019 Publication	1%
4	Ahmed A. Ansari, Junaid Ahmed, Hamza Arif, Aashir Iqbal, Hamza Asif Nizami, Yasar Ayaz.	1%

"Investigating Series-Parallel Actuation Arrangement in a Bioinspired Biped Robot", 2019 International Conference on Robotics and Automation in Industry (ICRAI), 2019
Publication

5	Uluc Saranli, Martin Buehler, Daniel E. Koditschek. "RHex: A Simple and Highly Mobile Hexapod Robot", The International Journal of Robotics Research, 2016 Publication	1 %
6	Neelima Mishra, Dinesh Goyal, Ashish Dutt Sharma. "Chapter 64 Design Process and Stress Analysis of Spine in Humanoid Serving Robot to Provide Proper Balancing and Load Bearing Capabilities", Springer Science and Business Media LLC, 2021 Publication	1 %
7	Aman Chaure, E Rajkumar. "Design, Analysis, Control and Manufacturing of a Head Massaging Machine", IOP Conference Series: Materials Science and Engineering, 2021 Publication	1 %
8	Will Bosworth, Sangbae Kim, Neville Hogan. "The MIT super mini cheetah: A small, low-cost quadrupedal robot for dynamic locomotion", 2015 IEEE International Symposium on Safety, Security, and Rescue Robotics (SSRR), 2015 Publication	1 %

9	M. Hutter, C. Gehring, A. Lauber, F. Gunther et al. "ANYmal - toward legged robots for harsh environments", Advanced Robotics, 2017 Publication	<1 %
10	Junwen Cui, Zhan Li, Jing Qiu, Tianxiao Li. "Fault-tolerant motion planning and generation of quadruped robots synthesised by posture optimization and whole body control", Complex & Intelligent Systems, 2022 Publication	<1 %
11	Marco Hutter, Christian Gehring, Dominic Jud, Andreas Lauber et al. "ANYmal - a highly mobile and dynamic quadrupedal robot", 2016 IEEE/RSJ International Conference on Intelligent Robots and Systems (IROS), 2016 Publication	<1 %
12	Daniel A. Tortorelli. "Sensitivity Analysis: Generalized Coordinate Kinematic Systems", CISM International Centre for Mechanical Sciences, 2009 Publication	<1 %
13	Nizar Rokbani, Seyedali Mirjalili, Mohamed Slim, Adel M. Alimi. "A beta salp swarm algorithm meta-heuristic for inverse kinematics and optimization", Applied Intelligence, 2022 Publication	<1 %

14	Waqas ur Rahman, Kwangsue Chung. "A Multi-path Based Adaptive Scheme for Multi-view Streaming over HTTP", IEEE Access, 2018 Publication	<1 %
15	Xingguo Song, Xiaolong Zhang, Xiangyin Meng, Chunjun Chen, Dashan Huang. "Gait optimization of step climbing for a hexapod robot", Journal of Field Robotics, 2021 Publication	<1 %
16	Baoping Ma, Yuefeng Rui, Chunlei Wang, Changwu Peng, Huishen Zhu, Xiaoqiang Li. "Research on Leg Transmission Mechanism of Quadruped Robot", 2021 6th International Conference on Control, Robotics and Cybernetics (CRC), 2021 Publication	<1 %
17	Springer Handbook of Robotics, 2016. Publication	<1 %
18	Ioannis Poulakakis, Madhusudhan Venkadesan, Shreyas Mandre, Mahesh M. Bandi et al. "Legged Robots with Bioinspired Morphology", Elsevier BV, 2017 Publication	<1 %
19	KangKyu Lee, Okkee Sim, Hyobin Jeong, Jaesung Oh, Hyoin Bae, Seungwoo Hong, Jun-Ho Oh. "Implementing Full-body Torque Control in Humanoid Robot with High Gear	<1 %

	Ratio Using Pulse Width Modulation Voltage", 2018 IEEE/RSJ International Conference on Intelligent Robots and Systems (IROS), 2018 Publication	
20	Katja Mombaur, Heike Vallery, Yue Hu, Jonas Buchli et al. "Control of Motion and Compliance", Elsevier BV, 2017 Publication	<1 %
21	"Humanoid Robotics: A Reference", Springer Science and Business Media LLC, 2019 Publication	<1 %

TABLE OF CONTENTS

LIST OF TABLES

LIST OF FIGURES

ABBREVIATIONS

ASLP	Advanced spring-loaded pantograph
SLP	Spring loaded pantograph
ELSM	Elastically Loaded Scissor Mechanism
EFLM	Elastic four-bar linkage mechanism
RPLM	Rigid parallel link mechanism
GRF	Ground reaction force
SLIP	Spring loaded inverted pendulum
HAA	Hip abduction/ adduction
HFE	Hip flexion/extension
KFE	Knee flexion/extension
COT	Cost of transport
DOF	Degree(s) of freedom
Fr	Froude number
SEA	Series Elastic Actuation
PEA	Parallel Elastic Actuation
ATRIAS	Assume the Robot is a Sphere
MABEL	Michigan Anthropomorphic Biped with Electronic Legs
IMU	Inertial Measurement Unit

NOMENCLATURE

F	Force
F_R	Reaction force
M	Moment
M_R	Reaction moment
σ	Normal stress
σ_s	Shearing stresses
σ_b	Bearing stresses
σ_B	Normal stress due to bending
I	Second moment of area
b	Base of area section
h	Height of area section
c	Point of interest for computing bending stresses
K	Stress concentration factor at holes
m	Mass
g	Gravitational acceleration
v	Velocity
K	Spring constant (N/m)
N_a	No. Of active coils of spring
P	Pitch (mm)
L_s	Solid length of spring
L_o	Free length of spring
d	Wire diameter
y_{max}	Maximum compression
n	Factor of safety
G	Shear modulus
C	Spring index
K_B	Bergsträsser factor

τ_{max}	Maximum shear stress
S_{sy}	Yield strength
S_{ut}	Ultimate tensile strength
α	Helix angle of spring
F_L	Applied load
M_L	Applied moment
L	Moment arm of applied load
F_B	Moment arm of bearing load
B	Moment arm of bearing load
F_M	Reaction load at motor collar

CHAPTER 1: INTRODUCTION

Motivation

The motivation to pursue this project is to design, analyze and fabricate a four-legged robot using a unique mechanism known as the Elastically Loaded Scissors Mechanism (ELSM) having a higher mechanical advantage that can achieve locomotion over discontinuous paths and isolated steps while conserving energy.

Also, to facilitate research and provide insight into the legged locomotion of animals by mimicking animal gaits and to further research in quadruped robotics at undergraduate level in NUST.

Problem Statement

To design, analyze, develop, and fabricate a Lightweight ELS Leg, with proximal actuation and compliance for energy storage.

Objectives

1. Literature Review and CAD Model of Mechanism
2. Structural Analysis and Prototype Development
3. Mathematical Modeling and Fabrication
4. Post-Fabrication Testing and Final Prototype Development

Locomotion in every mobile entity (living or non-living) can be broadly divided into ground, aerial and underwater locomotion. Within ground locomotion, distinction is made between legged, wheeled, and crawling locomotion.

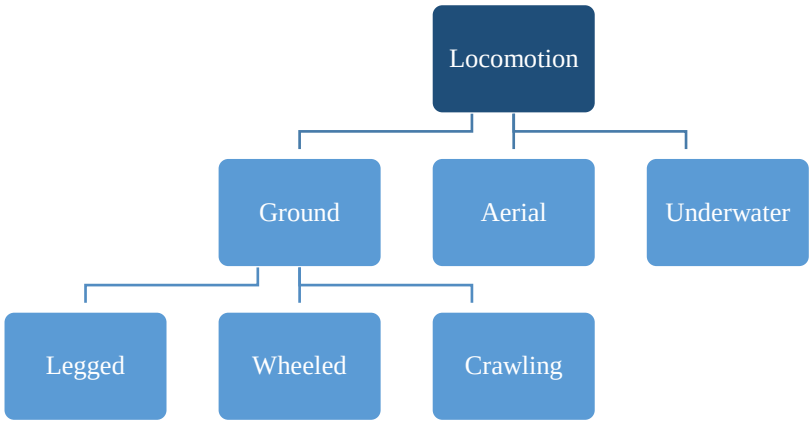

Figure 1: Types of Locomotion

Legged locomotion signifies all locomotion that is structured on legs and is exemplified by a multitude of biological creatures including mammals, insects, reptiles and birds. These animals possess variable degree of locomotion capabilities based on their leg morphology and size, number of joints and body posture.

Legged locomotion possesses several superior characteristics over wheeled locomotion. Since examples of wheeled locomotion are not found in nature, a comparison of legged and wheeled locomotion can be made in context of robotic locomotion.

In case of wheels, they are limited by their mobility by the requirement of continuous support pathways whereas legged locomotion can utilize isolated footholds or discontinuous pathways in order to overcome this limitation. This ability of theirs enable them to be much more useful in explorations. While wheels have to have sufficient

ground traction in order to move, articulated legs having adequate degrees of freedom (DOFs) are not limited by this requirement. This also reduces the friction and is more efficient than wheeled locomotion. Also, legs possess the ability to stabilize body posture, and reorient in case of a fall[1]. This comparison is presented in a pictorial form in Figure 2.

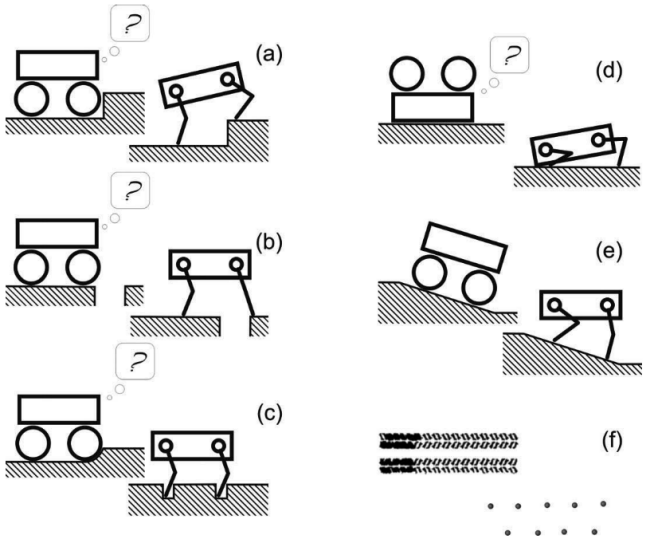

Figure 2: A comparison between wheeled and legged locomotion, image courtesy of [1]

Legs possess several remarkable functionalities. Their performance on rough terrains is demonstrated well by humans when they hike, and their agility is typified by animals like cheetah and ostrich. Legs with sufficient degrees of freedom allow the entity to move with different gaits; a horse can, for example, walk, ambling, trot, pace, and canter (or gallop) depending on speed and stability requirements[7]. The cyclic nature of legged movement allows for energy storage and release through spring-like elements in animal legs.

Figure 3: Stanford Doggo (left) and RHex (right)

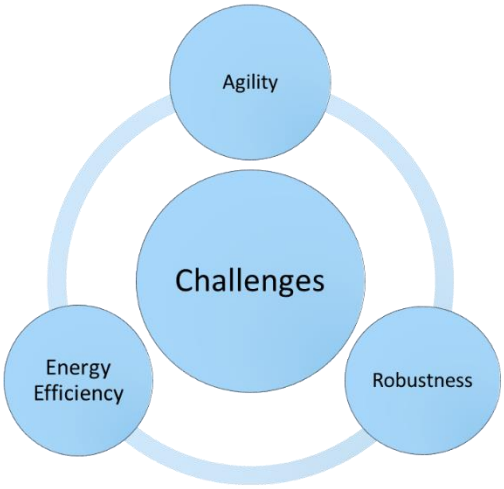

Figure 4: Challenges in legged robotics

Unlike legged animals, however, robots are faced with several challenges in the implementation of anthropomorphic leg concepts. Legged robots presenting agility, like the Stanford Doggo[8], do not possess sufficient DOF for dexterity and control but are highly energy-efficient. In contrast, the R- Hex[9] (Figure 3) is agile and functions well on unstructured terrains, but is not energy efficient. Figure 4 shows the challenges being faced in legged robotics.

The project presented in this report is a quadruped (four-legged) robot that is based on the Elastically Loaded Scissors (ELSM) to demonstrate the energy efficiency compared to the traditional Spring-Loaded Pantographs (SLP) based on observed examples in mammals. Legged robots require a tradeoff between the energy efficiency and power output or performance they provide. The quadruped robot is designed, based on the elastically loaded scissors mechanism in which the motor is connected to the proximal joint of the scissors using a pulley system as opposed to the distal joint in SLP. This proposed leg utilizes the increased mechanical advantage of the scissors mechanism to 'amplify' input angles to larger output displacement by the knee joint.

This report is structured so as to apprise the reader of the several biological, mechanical and actuation concepts in legged robotics and the existing models based on these concepts. The design procedure and complete design of the subject robot is then presented and explained in detail. Results of hitherto design exercises are then discussed and finally, conclusions, and possible additions and work in the future is presented.

CHAPTER 2: LITERATURE REVIEW

Legged robotics (and legged locomotion in general) is a field of study that exchanges information between biomechanics, control systems and mechatronics design. Several of the concepts in legged robotics are derived from observations from the biological world that can be qualitative or quantitative in nature. These concepts require hard grip on the above-mentioned fields.

Static vs Dynamic Locomotion

Research in legged locomotion began by the investigation of concepts of stability in motion. Static locomotion refers to motion in which the center of mass of the body is kept within the support polygon formed by its feet (or ground-contact points). Animals move with statically stable gait at slower speeds as shown in Figure 5.

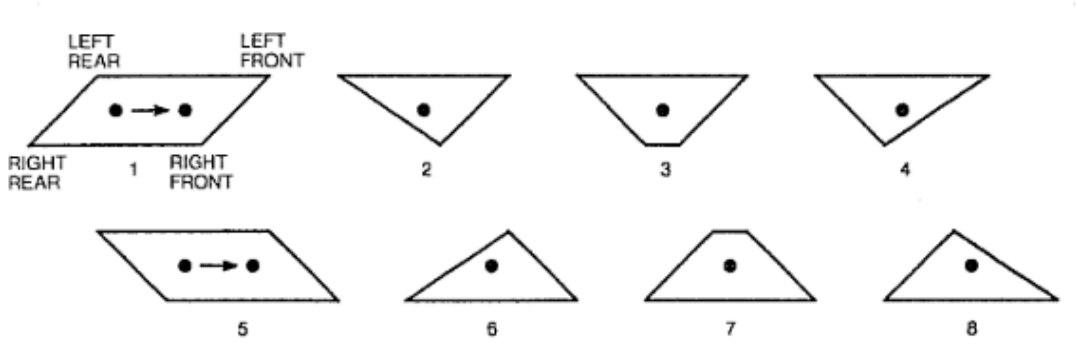

Figure 5: Sequence of support patterns for a crawling quadruped animal, adapted from [7]

Dynamic stability is explained best as momentary stable and ever-tipping motion in which the body is continuously falling and catching itself, on one leg (Raibert's One-Leg Hopper) or more than one leg (humans and animals). This periodic motion of falling and catching allows the body to move and accelerate

whilst keeping stable. Dynamic stability allows improved mobility and greater speeds[7]. A cheetah (Figure 6) performs high speed dynamic locomotion whilst chasing prey. When bounding, center of mass (COM) of the cheetah always lies outside of its support polygon, but the animal continues its motion with surprising elegance without falling over. This is due to the possessed momentum, which stabilizes the body before contact is made again, and the body propels itself forward; this is how repeated falling and catching works.

Figure 6: Cheetah with all its paws off the ground [1]

Much of Raibert's[7] earlier work was focused on dynamic locomotion, the proof-of-concept of which he demonstrated through his 3D One-Leg Hopper. This hopper consisted of a single telescopic pneumatically actuated leg connected to a torso at the hip, and as such was only capable of dynamic locomotion (since a single leg inherently prohibits static locomotion).

[1] https://qph.fs.quoracdn.net/main-qimg-ee5c4e33f18de95637615d3f6461de01

Template vs Anchor

The more complicated a system gets, the more involved its mathematical modeling becomes. Dynamics of legged locomotion are explained through the ideas of templates and anchors, first presented by Koditschek and Full[10].

A *template* is the simplest model that describes and predicts the behavior of an entity in pursuance of an objective. It is created by 'cutting away' all complexities such as joints, control neurons and muscles. The resulting model is accurate enough to explain the underlying physics and control requirements of the body.

The template of walking is described as the rotation of a rimless wheel (Figure 7) in which the legs act as rigid linkages incapable of changing length. During walking, one foot must always be in contact with the ground and ballistic flight does not occur. Walking and running are described by Froude number (Fr), which is a dimensionless ratio of centripetal and gravitational acceleration, that allows a size-independent comparison of animal and robotic locomotion.

$$Fr = \frac{centripetal\ acceleration}{gravitational\ acceleration} = \frac{v^2}{g \cdot l}$$

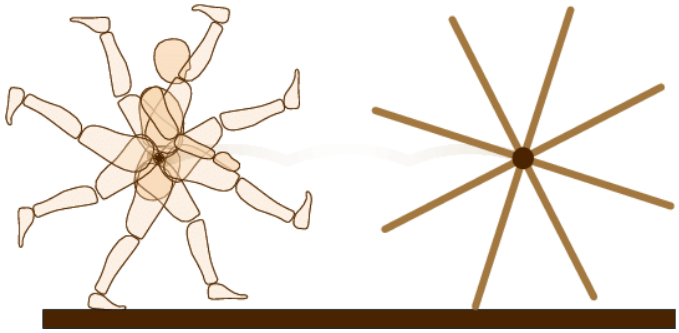

Figure 7: Walking is like rotation of a rimless wheel, adapted from [11]

At the value of $Fr > 1$, walking becomes physically impossible, and the gait has to be changed if speed is to be increased. Many animals switch from walking to running gaits at $Fr = 0.5$.

Running in animals is described by a spring loaded inverted pendulum (SLIP) template [12]possessing two distinct phases of stance and flight. In SLIP, a massless leg (spring) is connected to the body at the hip. The primary distinction between walking and running is that the leg is allowed to bend in running. This aspect is captured by the massless spring that changes its length depending on the loading. Refer to Figure 8 and Figure 9 for visualization of the SLIP model.

The two phases of running in SLIP motion, i.e. stance and flight are separated by the events of touch-down and lift-off of the foot and represent two dynamical systems: ground contact and ground reaction force (GRF) in stance phase, and gravity-driven ballistic motion in flight phase. This is known as hybrid dynamics.

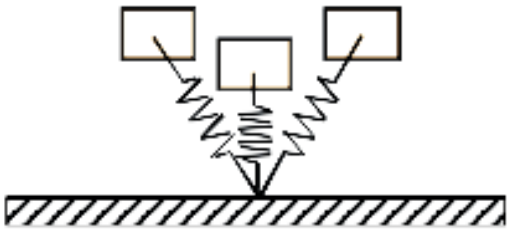

Figure 8: Running is modelled as SLIP motion

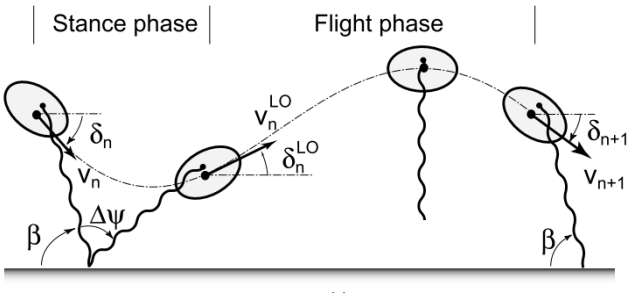

Figure 9: Stance and flight phases in SLIP motion, adapted from [12]

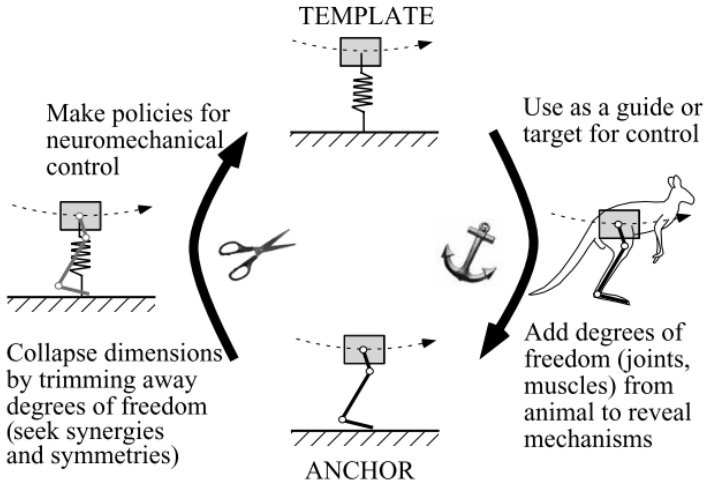

Figure 10: From anchors to templates, adapted from[10]

As much as templates are easier to understand and visualize, they reduce the accuracy of the mathematical model to some extent. The addition of actual limb morphology and physical details converts the template into an *anchor*. Figure 10 explains this transformation. The anchor, therefore, more closely resembles the functioning of articulated legs with several DOFs and actuators. It is easy to model a mechanism as an anchor in the flight phase but becomes much harder in the stance phase, in which the mechanism is modelled as the SLIP template. In Raibert's 3D One-Leg Hopper, the leg

mechanism closely resembles the SLIP template and therefore, both the template and anchor may be considered to be the same.

As described earlier, walking makes use of relatively stiffer legs which do not change their effective length (hip to foot) whereas running utilizes larger flexion and extension of all leg joints and is modelled as a spring. Therefore, hopping is considered a precursor to running and many of the energy storage and recovery concepts can be more lucidly understood through the study of hopping.

Springs

One of the ideas emanating from the cyclic nature of legged locomotion is the utilization of springs to store and release energy at various durations within each cycle. Animal legs are unique insomuch that the combination of muscles, tendons, and ligaments (and other biological entities) function together to do the work of actuation, energy storage and energy dissipation. These function in an articulated mechanism are mimicked using actuators, springs, and dampers.

Consider a mass that has to oscillate between two points on a horizontal line: one method would be to continuously power this movement; the other method would be to introduce a spring and connect it to the mass, displace the mass once and let the spring oscillate the mass between the points. Ideally, in absence of losses, a one-time displacement achieves the desired motion. This concept is being utilized in springs in animal bodies.

Alexander[14] has outlined three major bioinspired uses of springs in legged locomotion. These same uses can be extended to robotic legged locomotion:

1. Acting in the line of effective leg (virtual leg between foot and hip; regardless of leg morphology). This placement stores the negative work done on the actuator and then restores it to the leg.

2. Acting between leg and body at hip joint and getting engaged only when leg is off the ground. This arrangement is expected to help particularly when the robot is running at high speeds.
3. As foot pads to reduce the impact force by increasing duration of foot deceleration. Chattering[15], which is high frequency oscillation, occurs at the foot, if these foot pads are absent.

Alexander[16] also reports that most of the energy storage occurs distal to the knee in animals. The Achilles tendon functions as an energy storage element between the thigh and the ankle. This tendon also reduces the GRF on impact.

Springs, as passive mechanical elements, contribute to passive dynamics. Hutter[17] states that robots can be made energetically efficient by letting the passive system dynamics drive the motion and that active actuation should only be done to shape and preserve the motion.

Actuators

A mechanical hopping system with leg limbs connected to each other with connection components such as screws, nuts, washers and sleeves, has some amount of Coulomb friction damping, which causes the conversion of kinetic energy of the limbs into heat which is wasted in the surroundings causing a continuous decrement in the hopping height of the system. To ensure sustainable hopping gait and height, the limbs are actuated to compensate for the loss of energy by providing additional torque to the leg limbs.

Arumugom et al.[18] have explored and compared the different control and actuation techniques for robots. The robots which are used in a bounded environment for a specific task or to reach a specific position repeatedly throughout its life, such as a robotic arm working in an assembly line of a

factory, requires position control of its end effector. For an unbounded and irregular terrain, the position control of a hopping robot is more difficult to achieve because of the varying target positions for the robot foot to land at. That is why, force control with actuators is applied on such robots. A comparison of actuators is stated as below:

1. Geared actuators have significant amount of back-lash and static friction, thus greater energy losses.
2. Pneumatic actuators are difficult to position-control and have less power delivering capacity.
3. Fluidic muscles have hysteresis, small stroke to length ratio and a non-linear response.
4. Hydraulic actuators have deficient back drivability despite of their good power to weight ratio.

Two configurations of elastic actuation are most commonly used in legged robotics. These are:

- Series Elastic Actuation (SEA): A spring is placed in series between the actuator and load. This configuration ensures isolation of shock on the load from the actuator. In this way actuator remains safe from impact forces. Force control is achieved in SEA due to the deformation of spring; however, position control is lost.
- Parallel Elastic Actuation (PEA): The actuator and spring are placed parallel to each other and connected to the load directly. Precise position control of the load can be achieved due to rigid connection of actuator with the spring. Force control is lost in this configuration.

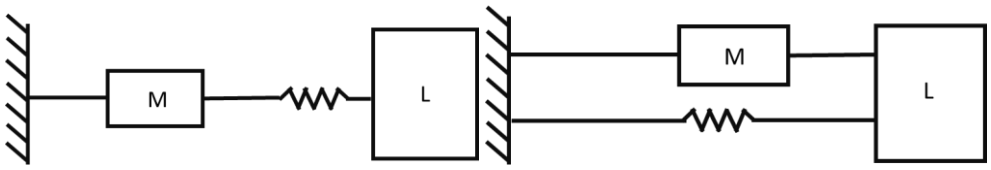

Figure 11: SEA (left) and PEA (right) configuration

Memorable works

Due to the growth of bio robotics, the work and research in this field has led to a number of robots. The dictations of the aforementioned design objectives lead us to investigate them. Here are a few mentionable works in this domain:

1) Stanford Doggo

Built by Stanford University, the Stanford Doggo[3] is a quadruped robot which features a QDD transmission. This improves upon the mechanical design of another quadruped robot with a similar leg linkage design, Minitaur. In the Minitaur, the two motors used to control each leg are mounted on either side of the leg linkage. However, the structural element connecting these two motors prevents the leg from completing a full revolution and limits the workspace of the robot. On the other hand, this robot uses coaxial drive assemblies which allow the legs to rotate outside of the body (without any constraints) (Figure 13). Each such coaxial drive assembly consists of two belt drives in a 3:1 ratio, which enable power to be transferred from the motors to the drive shafts. The two drive shafts nest inside each other coaxially which, in addition to saving weight and space, also allows the leg to rotate in either direction continuously.

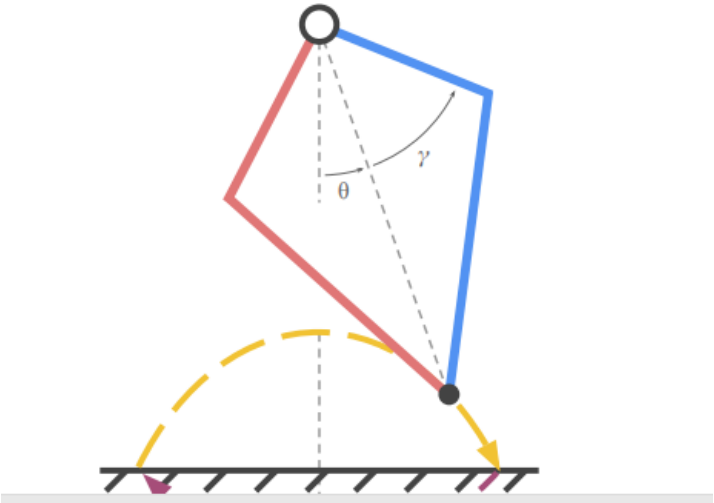

Figure 12: Leg design for Stanford Doggo, adapted from [3]

2) Super Mini Cheetah

The Super Mini Cheetah[4] robot was made with commercial electromechanical components. In an effort to reduce cost and increase replicability, its manufacturers used modern rapid prototyping methods. The robot leg's ability to perform force and impedance control during locomotion was shown. The benefit of such limbs which can use force and impedance control is made clear by the wide range of locomotion behaviors that were demonstrated by the robot with a very simple design methodology. This ability to use different gaits for locomotion enables the experiments to be carried out on various types of environments and terrains.

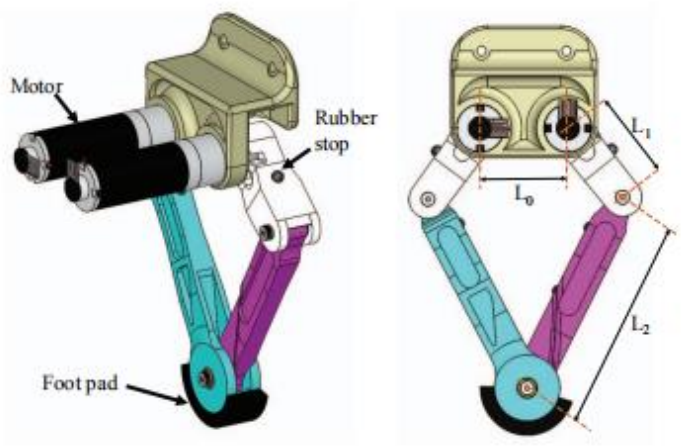

Figure 13: Super Mini Cheetah leg design, adapted from [4]

3) StarlETH

StarlETH [17] is based on a quadruped mammal and utilizes three motors which are termed as HAA (hip abduction/ adduction), HFE (hip flexion/ extension) and KFE (knee flexion/ extension). It consists of serial leg linkages that represent a mammalian thigh and shank with a ball foot at its end; the legs do not have an ankle joint and thus consist of 3 DOF only (thigh roll, thigh pitch & knee pitch).

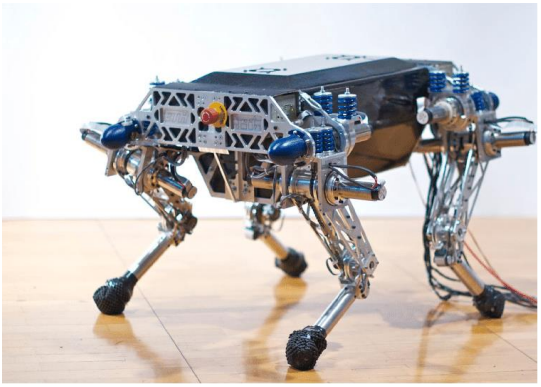

Figure 14: **StarlETH (now ANYmal, left) [17] and Cheetah-cub (right)**

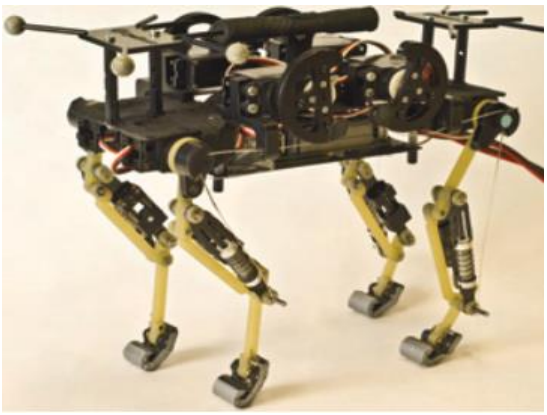

Figure 15: StarlETH (now ANYmal, left) [17] and Cheetah-cub (right) [19]

Spring placement for energy storage and recovery in StarlETH is dictated by mechanical design considerations rather than anthropomorphic observations. The knee joint is actuated through a chain-sprocket mechanism by a motor placed at the torso; a spring grounded at the torso and driven from the driving sprocket stores the energy of knee flexion and extension. Motor placement and the driving mechanism allows the robot to achieve different leg configurations other than the 'X' configuration shown in Figure.

4) RHex

RHex [20] has only six actuators in its body, with one motor situated on each hip. It achieves the mechanical simplicity that enables a reliable and robust operation while carrying out real-world tasks. Empirically, stable and highly maneuverable locomotion is based on a very simple clock-driven, open-loop tripod gait. The legs rotate full circle, thus avoiding the common problem of toe stubbing in the protraction (swing) phase. A wide range of experimental results document the robot's significant "intrinsic mobility" - the traversal of rugged, broken, and obstacle-ridden ground without any terrain sensing or actively controlled adaptation. R Hex is capable of fast and robust forward locomotion

while traveling at speeds up to one body length per second, in addition to traversing height variations well exceeding its body clearance.

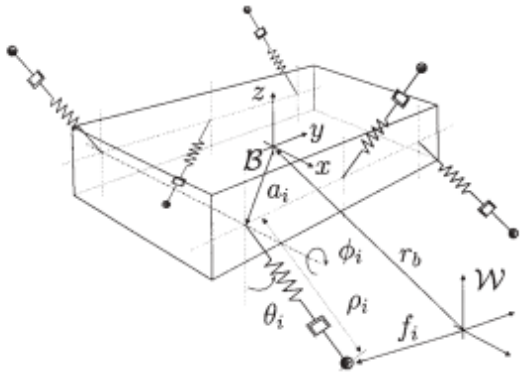

Figure 16: R Hex simple mechanism, adapted from [20]

5) Ghost Minitaur

Ghost Minitaur can best be described as a dynamically running and leaping quadruped robot [21]. It is a part of a new class of legged robots that are based on direct drive (DD). The benefits of the DD robot design include increased specific power, transparency, increased mechanical robustness / efficiency, and high actuation bandwidth. Thus, it enables behaviors which are highly energetic despite the presence of severe limitations as far as specific force is concerned.

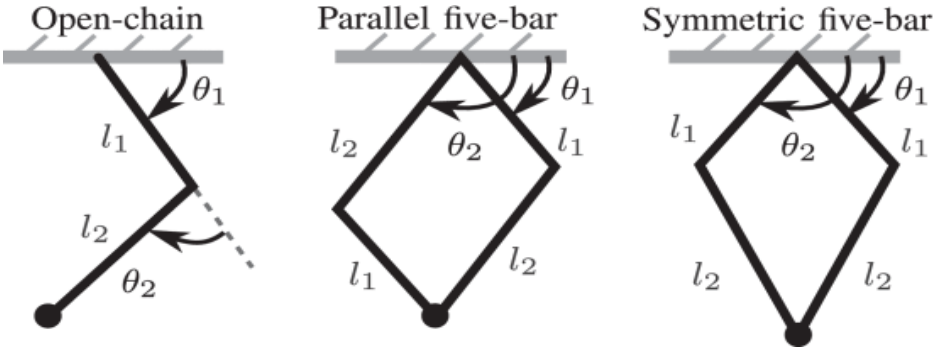

Figure 17: Comparison of chain mechanism for Ghost Minitaur, adapted from [5]

6) ANYmal

ANYmal[22] is a part of a class of robots that are capable of high mobility with dynamic locomotion. In its design phase, the objective was to create system which was both rugged and easy to maintain. The manufacturers achieved this with the use of modular joint units called ANYdrive, which enable the easy production of robots with a different kinematic structure. In case the robot fails, these units were simple to replace. These actuators are based on a series elastic concept which had already been implemented on the StarlETH robot (mentioned above). Experiments were carried out and the results supported the designers' claim of robustness. Not a single gearbox failure was reported in four years of operation. This, along with a large variety of motion enables the robot to carry out several maneuvers to stand up after falling down or to overcome obstacles which may be present in its path. Since there are less constraints related to internal systems, motion planning is made easier. Several experiments carried out during the preliminary phase, such as dynamic trotting, careful stair climbing, and ZMP-based walking proved successful. More complex operations, such as search and rescue or industrial inspection, will be investigated in the next phase of development.

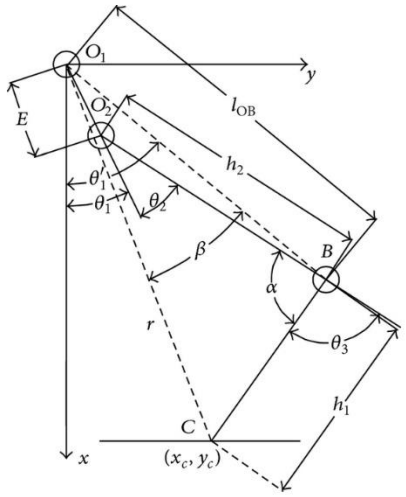

Figure 18: Leg mechanism of ANYmal, adapted from[6]

Spring Loaded Pantographs (SLP)

Spring Loaded Pantographs (SLPs) are frequently used in designing lightweight limbs for multi-legged robots. Quadruped robots that incorporate cable pulled SLP legs have proven to be agile, robust, and capable of conserving energy during their gait cycle. In such designs, the extension of the distal segments via the knee joint is dependent upon the length of the cable. [29]

A biologically inspired method of leg actuation is by the usage of a mechanism called Spring Loaded Pantographs (SLPs). The intuition behind the usage of pantographs is bio-inspired as studies have indicated that mammals mostly tend to keep the proximal and distal segments parallel during the gait cycle [25]. Sprowitz et. al. demonstrated the application of Advanced Spring-Loaded Pantograph (ASLP), a variant of the SLP, in Cheetah-Cub [26] and Oncilla Robots [27] as they achieved dynamic trot gait. Although, it is possible to achieve the same parallel-angle behavior by using actuated pin knee joints, but that would add a further layer of control complexity that can otherwise be removed by using the SLP approach. One of the advantages of the SLP mechanism is that it makes it possible to actuate the leg via a cable which enables the actuators to be mounted onto the body and hence reducing the leg mass and inertia properties. Secondly, during stance stage, when the leg is in contact with the ground, the cable `sags', bypassing the actuator and making the load in series with spring. This makes the actuator decoupled from the dynamics of the legged robot and dependent upon the energy stored in the spring.

One feature of the cable pulled SLP mechanism is that length of the thread required to actuate the knee joint is rolled onto a pulley whose diameter is directly proportional to the length of the rolled cable. This means that in order to significantly retract the knee joint, a larger diameter pulley is required, otherwise the reach of the leg, and hence its ability to

traverse uneven terrains and to reject disturbances from the ground is compromised. This would further affect the weight as the robot is scaled up for larger practical applications.

The efficiency in terms of output motion of the SLP mechanism can be improved by replacing the pantographic mechanism with a scissor's mechanism.

Elastically Loaded Scissors Mechanism (ELSM)

The Elastically Loaded Scissors Mechanism (ELSM) is considered a better alternative to the SLP because of its higher mechanical advantage, compact design, and parallel segment property.

This mechanism does not affect the overall power transmission, it just varies the torque velocity ratio. Another advantage of scissor's transmission over traditional gear transmissions is that it does not get affected by backlash. Furthermore, the ELS mechanism requires less thread to be rolled onto the actuator pulley as compared to the SLP mechanism for the same amount of knee joint retraction (high mechanical advantage). If servo motors are used, as was done in the EPFL cheetah robot [26], [28], the rotational velocity saturates at a certain threshold value. Using the mechanical advantage of the scissor's mechanism higher output range of motion is attainable for lower input range of motion. This enables to `harvest' higher step-down velocities of the foot as compared to the SLP design. [29]

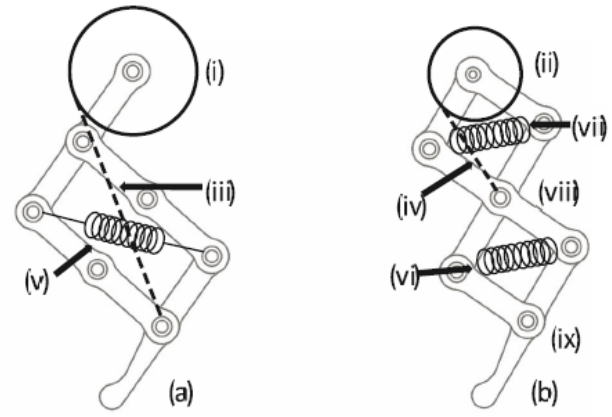

Figure 15: The Spring-Loaded Pantograph (a) and Elastically Loaded Scissors (b) configurations considered. (i) and (ii) are pulleys, (iii) and (iv) represent the cable threads, (v), (vi) and (vii) represent elastic elements, (viii) represents the proximal joint and (ix) represents the distal joint.

CHAPTER 3: METHODOLOGY

Design Inspiration

The leg design finalized for our quadruped robot derives strong inspiration from other famous quadruped robots, such as the Ghost Robotics' Ghost Minitaur, Stanford's Doggo and MIT's Super-Mini Cheetah. Other more complex designs were also studied during our Literature Review but were ultimately discarded due to the increased cost of manufacturing and unavailability of high quality and precise manufacturing techniques. After considering numerous factors such as cost, manufacturing limitations and design limitations our final design was a unique blend of some aspects of a Stanford's Doggo and other aspects of a scissor lift mechanism. This resulted in a 6-bar mechanism that, which when fitted with a pulley system and elastic elements resulted in efficient leg retraction and expansion. The process of dimensioning was iterative, taking maximum torque and structural considerations, such as the total weight of the assembly, into account.

Table 1: Link Lengths

Link	Length (mm)	Thickness (mm)
L_1	34	5
L_2	34	5
L_3	68	5
L_4	68	5
L_5	34	5

L_6	68	5

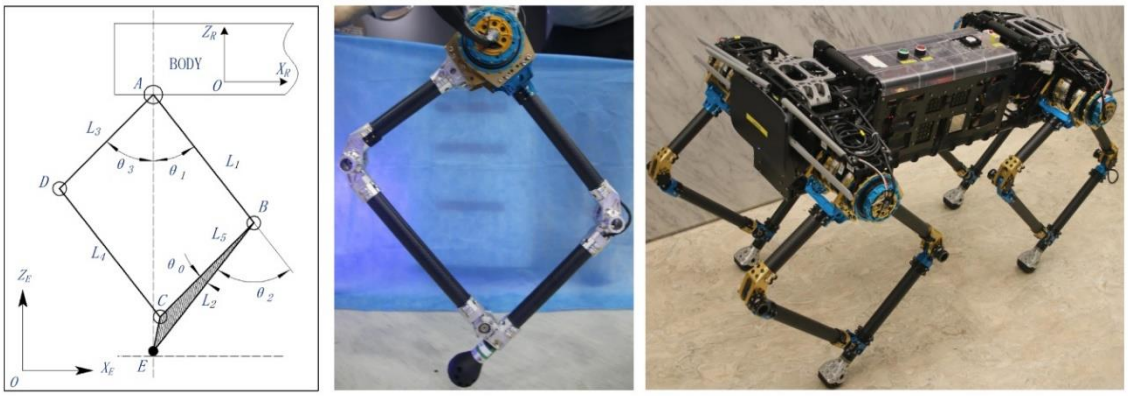

Figure 16: Stanford Dog

Forward Kinematics:

The following rules were employed for the assignment of the Denavit-Hartenberg (DH) frames:

- a_i is the distance from Z_{i-1} to Z_i measured along X_i
- α_i is the angle from Z_{i-1} to Z_i measured about X_i
- d_i is the distance from X_i to X_{i+1} measured along Z_i
- θ_i is the angle from X_i to X_{i+1} measured about Z_i

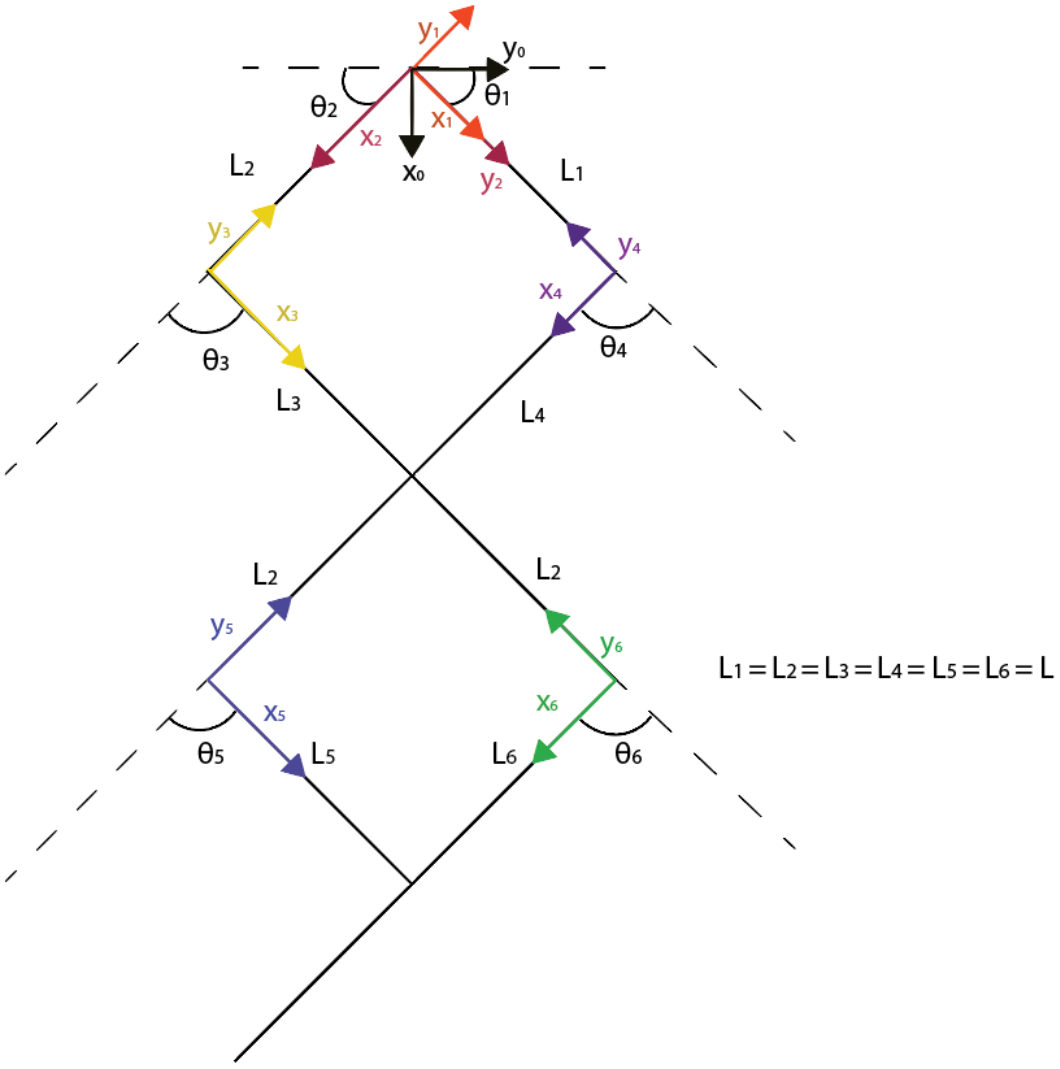

Figure 17: Frame Assignments

The DH table constructed from this frame assignment is shown below:

Table 2: DH Table

i	a_{i-1}	α_{i-1}	d_i	θ_i
1	0	0	0	θ_1
2	0	180^o	0	$180^o - 2\theta_1$
3	L	180^o	0	θ_3
4	0	180^o	0	θ_4
5	$2L$	180^o	0	θ_5
6	0	180^o	0	θ_6

Inputting the data taken from the table 2 into the Forward Kinematics MATLAB code in Appendix II, we attain the transformation matrices for each link. Multiplying these links results in the final matrix relating the position of the end effector with respect to the base, i.e.

$$^0_6T = {}^0_1T \cdot {}^1_2T \cdot {}^2_3T \cdot {}^3_4T \cdot {}^4_5T \cdot {}^5_6T$$

The final transformation matrix attained from MATLAB is:

$$\begin{pmatrix} \sigma_3 + \sigma_2 & \sigma_1 & 0 & L\,\sigma_8 + 2\,L\,\sigma_7 \\ \sigma_1 & -\sigma_3 - \sigma_2 & 0 & L\,\sigma_9 + 2\,L\,\sigma_6 \\ 0 & 0 & -1 & 0 \\ 0 & 0 & 0 & 1 \end{pmatrix}$$

Figure 18: Final Transformation Matrix

where

$$\sigma_1 = \cos\left(\frac{\pi\ \text{thet}_6}{180}\right)\sigma_4 - \sin\left(\frac{\pi\ \text{thet}_6}{180}\right)\sigma_5$$

$$\sigma_2 = \sin\left(\frac{\pi\ \text{thet}_6}{180}\right)\sigma_4$$

$$\sigma_3 = \cos\left(\frac{\pi\ \text{thet}_6}{180}\right)\sigma_5$$

$$\sigma_4 = \cos\left(\frac{\pi\ \text{thet}_5}{180}\right)\sigma_6 + \sin\left(\frac{\pi\ \text{thet}_5}{180}\right)\sigma_7$$

$$\sigma_5 = \cos\left(\frac{\pi\ \text{thet}_5}{180}\right)\sigma_7 - \sin\left(\frac{\pi\ \text{thet}_5}{180}\right)\sigma_6$$

$$\sigma_6 = \cos\left(\frac{\pi\ \text{thet}_3}{180}\right)\left(\cos\left(\frac{\pi\ \text{thet}_3}{180}\right)\sigma_9 + \sin\left(\frac{\pi\ \text{thet}_3}{180}\right)\sigma_8\right) - \sin\left(\frac{\pi\ \text{thet}_3}{180}\right)\left(\cos\left(\frac{\pi\ \text{thet}_3}{180}\right)\sigma_8 - \sin\left(\frac{\pi\ \text{thet}_3}{180}\right)\sigma_9\right)$$

$$\sigma_7 = \cos\left(\frac{\pi\ \text{thet}_3}{180}\right)\left(\cos\left(\frac{\pi\ \text{thet}_3}{180}\right)\sigma_8 - \sin\left(\frac{\pi\ \text{thet}_3}{180}\right)\sigma_9\right) + \sin\left(\frac{\pi\ \text{thet}_3}{180}\right)\left(\cos\left(\frac{\pi\ \text{thet}_3}{180}\right)\sigma_9 + \sin\left(\frac{\pi\ \text{thet}_3}{180}\right)\sigma_8\right)$$

$$\sigma_8 = \cos\left(\frac{\pi\ (2\ \text{thet}_1 - 180)}{180}\right)\cos\left(\frac{\pi\ \text{thet}_1}{180}\right) - \sin\left(\frac{\pi\ (2\ \text{thet}_1 - 180)}{180}\right)\sin\left(\frac{\pi\ \text{thet}_1}{180}\right)$$

$$\sigma_9 = \cos\left(\frac{\pi\ (2\ \text{thet}_1 - 180)}{180}\right)\sin\left(\frac{\pi\ \text{thet}_1}{180}\right) + \sin\left(\frac{\pi\ (2\ \text{thet}_1 - 180)}{180}\right)\cos\left(\frac{\pi\ \text{thet}_1}{180}\right)$$

Hence, the final frame coordinates are determined as follows:

$$\begin{pmatrix} L\,\sigma_5 + 2\,L\,\sigma_4 + \text{bx}\,\sigma_2 + \text{by}\,\sigma_1 \\ L\,\sigma_6 + 2\,L\,\sigma_3 + \text{bx}\,\sigma_1 - \text{by}\,\sigma_2 \\ -\text{bz} \\ 1 \end{pmatrix}$$

where

$$\sigma_1 = \cos\left(\frac{\pi\ \text{thet}_6}{180}\right)\ \left(\cos\left(\frac{\pi\ \text{thet}_5}{180}\right)\sigma_3 + \sin\left(\frac{\pi\ \text{thet}_5}{180}\right)\sigma_4\right) - \sin\left(\frac{\pi\ \text{thet}_6}{180}\right)\ \left(\cos\left(\frac{\pi\ \text{thet}_5}{180}\right)\sigma_4 - \sin\left(\frac{\pi\ \text{thet}_5}{180}\right)\sigma_3\right)$$

$$\sigma_2 = \cos\left(\frac{\pi\ \text{thet}_6}{180}\right)\ \left(\cos\left(\frac{\pi\ \text{thet}_5}{180}\right)\sigma_4 - \sin\left(\frac{\pi\ \text{thet}_5}{180}\right)\sigma_3\right) + \sin\left(\frac{\pi\ \text{thet}_6}{180}\right)\ \left(\cos\left(\frac{\pi\ \text{thet}_5}{180}\right)\sigma_3 + \sin\left(\frac{\pi\ \text{thet}_5}{180}\right)\sigma_4\right)$$

$$\sigma_3 = \cos\left(\frac{\pi\ \text{thet}_3}{180}\right)\ \left(\cos\left(\frac{\pi\ \text{thet}_3}{180}\right)\sigma_6 + \sin\left(\frac{\pi\ \text{thet}_3}{180}\right)\sigma_5\right) - \sin\left(\frac{\pi\ \text{thet}_3}{180}\right)\ \left(\cos\left(\frac{\pi\ \text{thet}_3}{180}\right)\sigma_5 - \sin\left(\frac{\pi\ \text{thet}_3}{180}\right)\sigma_6\right)$$

$$\sigma_4 = \cos\left(\frac{\pi\ \text{thet}_3}{180}\right)\ \left(\cos\left(\frac{\pi\ \text{thet}_3}{180}\right)\sigma_5 - \sin\left(\frac{\pi\ \text{thet}_3}{180}\right)\sigma_6\right) + \sin\left(\frac{\pi\ \text{thet}_3}{180}\right)\ \left(\cos\left(\frac{\pi\ \text{thet}_3}{180}\right)\sigma_6 + \sin\left(\frac{\pi\ \text{thet}_3}{180}\right)\sigma_5\right)$$

$$\sigma_5 = \cos\left(\frac{\pi\ (2\ \text{thet}_1 - 180)}{180}\right)\cos\left(\frac{\pi\ \text{thet}_1}{180}\right) - \sin\left(\frac{\pi\ (2\ \text{thet}_1 - 180)}{180}\right)\sin\left(\frac{\pi\ \text{thet}_1}{180}\right)$$

$$\sigma_6 = \cos\left(\frac{\pi\ (2\ \text{thet}_1 - 180)}{180}\right)\sin\left(\frac{\pi\ \text{thet}_1}{180}\right) + \sin\left(\frac{\pi\ (2\ \text{thet}_1 - 180)}{180}\right)\cos\left(\frac{\pi\ \text{thet}_1}{180}\right)$$

Inverse Kinematics:

We used symmetry to simplify the 6-DOF leg to a 3-DOF linkage. The detailed inverse kinematics calculations have been discussed in Appendix II. Hence, given the parameters x, y and l, we can determine the following angles of the robot:

Table 3: Inverse Kinematics Results

Parameter	Formula
φ_1	$\sin^{-1}\left(\frac{\mathrm{y} - 4l\sqrt{\frac{l^2 - x^2}{l^2}}}{l}\right)$
φ_2	$2\cos^{-1}\left(\frac{x}{l}\right)$

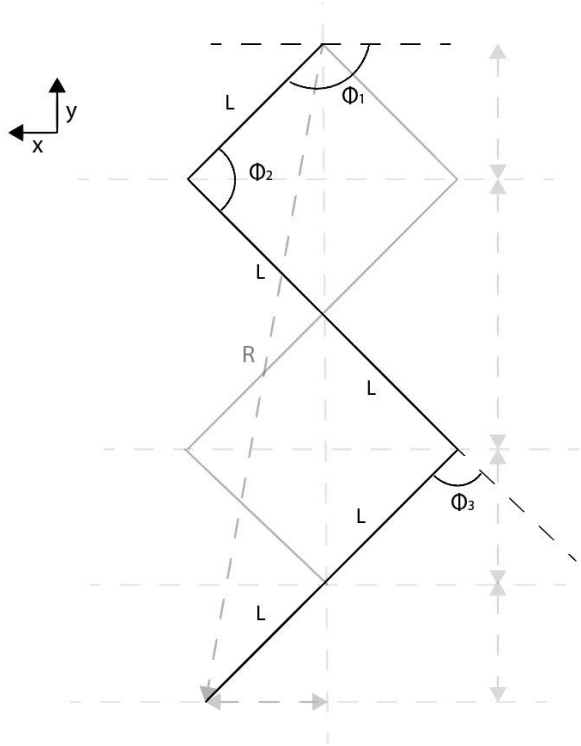

Figure 19: Inverse Kinematics Diagram

Actuator Selection

For the selection of the motors, appropriate torque calculations were conducted to determine the required torque and hence the servo motor that would fulfil this requirement. After a detailed market survey, where multiple servo motors were considered and a cost-benefit analysis was conducted, the Tower Pro MG996R servo motor was finalized as it gave the closest numbers to our requirement while remaining within our cost requirement.

Figure 20: TWR Pro MG 996R

The Tower Pro MG996R provides has a weight of 55 grams and operates between $4.8\,V$ and $7.2\,V$. Moreover, it has a stall torque of $9.4\,kgf.cm$ and can rotate a total of 120^o, 60^o in each direction. Following table describes the further details regarding the selected actuator.

Table 4: MG TWR Pro MG 996R Specifications

Specification	Details
Weight	55 grams
Operating Voltage	4.8V – 7.2V
Running Current	500 mA – 900 mA
Stall Current	2.5 A
Stall Torque	9.4 kgf·cm (4.8 V), 11 kgf·cm (6 V)
Temperature Range	0℃ – 55℃

Actuator Placement

The design finalized for this project required two elastic elements to be attached above and below the proximal (knee) joint. These elastic elements, in combination with the symmetry of the leg design provided by the presence of the scissor mechanism, allowed the control of the retraction of the leg to become extremely simple. A pulley mechanism attached on top of the leg, connecting itself to the proximal joint would be sufficient actuation for complete retraction and expansion of the leg.

However, another actuator was required to control the swing of the leg that would allow for locomotion to take place. The placement of this actuator is at the point where links L_1 and L_2 meet. Control over this point of the leg, through a servo motor would provide the leg with 120^o of rotational motion, 60^o on either side.

Hence, both actuators can be placed on top of the leg, with one controlling the leg in its swing phase and the other controlling it in its retraction and expansion phase.

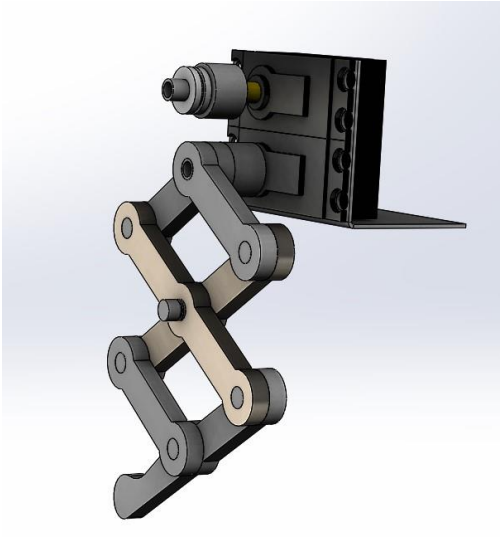

Figure 21: Prototype Assembly

Similarly, the prototype for testing purposes was assembled as shown above.

Material Selection:

After consultations among ourselves and other students who have partaken in robotics projects, we decided to reject Aluminum and Steel due to weight concerns and technical issues with their machining, pertaining to tolerancing and availability of service providers. 3D printing or laser cutting were the best options for us, considering our requirements and design. Therefore, we had to choose between ABS and Acrylic. The surprising rarity of ABS in the Rawalpindi/Islamabad and Karachi marketplace made the decision of choosing Acrylic very easy as it met the tensile strength and weight requirements that we deemed necessary due to our calculations and simulations. Hence, acrylic was chosen for the manufacture of each of the links.

Table 5: Material Comparison

Material	Young Elastic Modulus (GPa)	Density (kgm^{-3})	Tensile yield strength (MPa)	Ultimate tensile strength (MPa)	Hardness	Shear strength (MPa)	Moisture absorption %
Steel 1018	190	7900	240-400	430-480	71 (B)	----	---
Aluminum 6061-T6	69	2700	276	310	60(B)	207	---
ABS (molded)	0.778-6.10	882-3500	20-77	2.6-73.1	90 (R)	---	0.02-2.3
Acrylic	0.95-3.79	700-1300	25-85	19.3-80.5	40-54 (R)	---	0.3-0.6
Nylon 6	1.3-4.2	1110-1170	40-100	50-90	100-120(R)	44.8-75.8	0.3-7

The pulley used above the leg is to be manufactured from nylon. Nylon, with its ease of availability of material and of manufacturing service providers, made it an obvious choice for the simple design of the pulley. The nuts and bolts are the standard stainless-steel type that are widely available in the market.

Manufacturing

- Leg Links Manufacturing

The links of the robots are made of acrylic and were laser cut from 6 mm sheets of acrylic. Laser cutting was chosen as it was the most time-efficient method, more so that 3D printing, and the design of our leg was simple enough that laser printing each link separately sufficed and 3D printing was not necessary.

Figure 22: Laser Cut Links

Similarly, the base plate for the quadruped has been designed on the SolidWorks and manufactured via same laser cutting operation. Same acrylic sheet has been used to cut the base plate for quadruped.

- Pulley System Design

In order to complete the prototype assembly, a pulley system design to control the distal joint via a second actuator was designed. The pulley was designed on the SolidWorks and manufactured using a nylon tube via lathe operations. A stainless-steel screw was then used to couple the nylon pulley to the actuator shaft. The pulley to be fitted on the actuator on top of the leg is to be made of nylon and is a very simple, short cylinder. This part of the robot can be easily manufactured on a lathe machine in MRC.

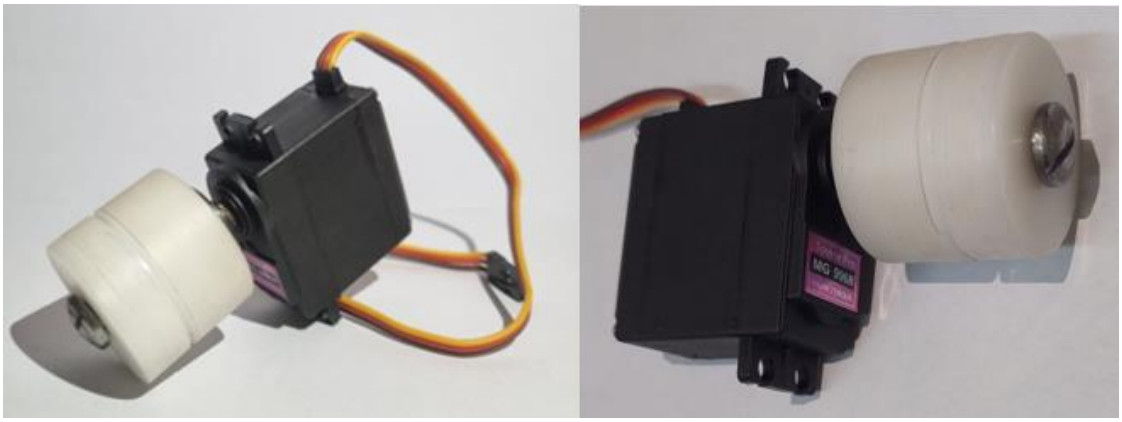

Figure 23: Nylon Pulley and Actuator Coupling

- Threaded Sleeves and Screws for Link Joints

These links were assembled using a combination of a threaded sleeve nut with a bolt. A M30 internally threaded sleeve nut was used to fit a M30 threaded bolt.

Figure 24: Threaded Sleeve and Screw

- Aluminum Brackets

Finally, the bracket to hold the actuators and the body of the robot, that will hold the electrical equipment is to be made of aluminum 6061-T6 alloy. This part requires structural rigidity and hence compromises cannot be made on the strength of the material to allow for reduced weight. Therefore, the body will an Aluminum 6061-T6 alloy sheet that is widely available in the market and is very easy to work on.

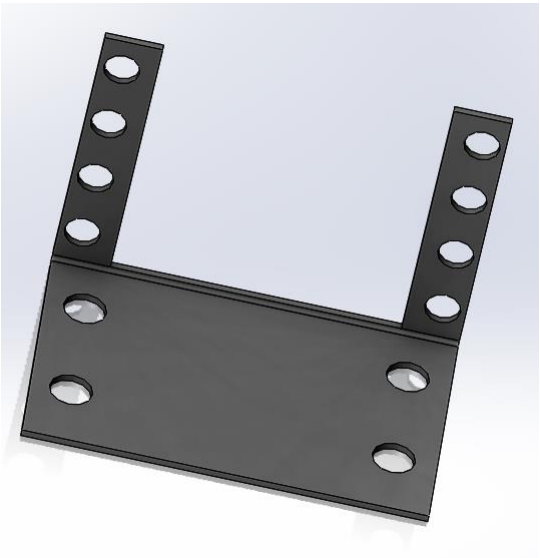

Figure 25: Aluminum Brackets Designed on SolidWorks

- Prototype Assembly

After successful fabrication of different required components, a small prototype i.e., the one leg of the quadruped was assembled for testing and trials. A fishnet thread has been incorporated for coupling the distal joint with the pulley.

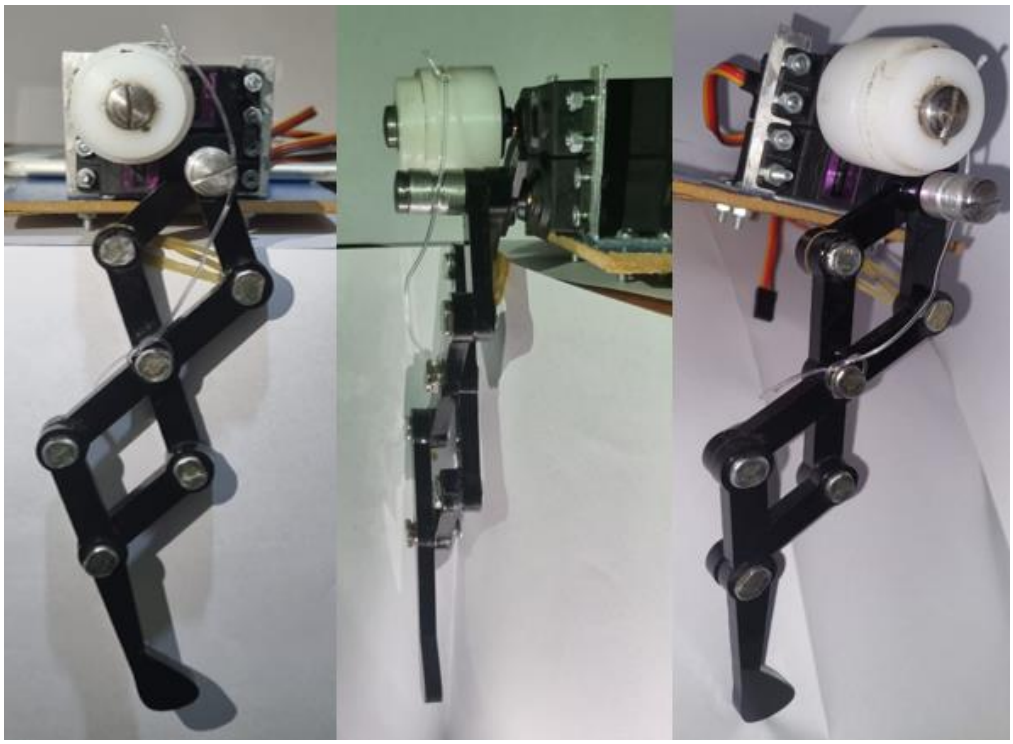

Figure 26: Assembled Prototype (front, side, and isometric views)

- Base Plate Design

The next step after the successful fabrication and testing was to pre-analyze the manufacturing and fabrication of the whole quadruped. The first step in the final assembly of the quadruped is the design of the base plate to mount the actuators and control system for the legs. The design of the base plate has been done on SolidWorks

and manufacturing has been done using the laser cutting technique. Similar to the link legs, acrylic plate has been used for the base plate.

Table 6: Base Plate Dimensions

Length	200 mm
Width	120 mm
Thickness	5 mm

Following figures show the designed base plate and the actual laser cut result from the acrylic sheet.

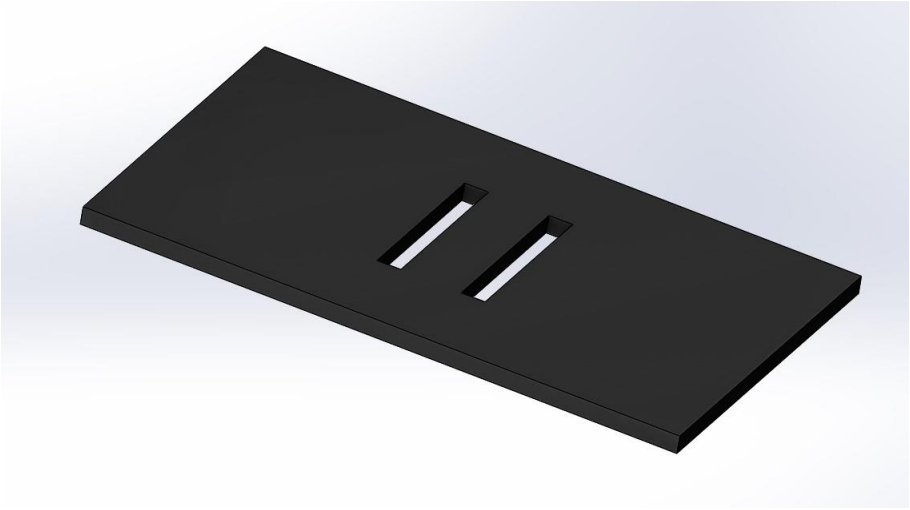

Figure 27: Designed Base Plate on SolidWorks

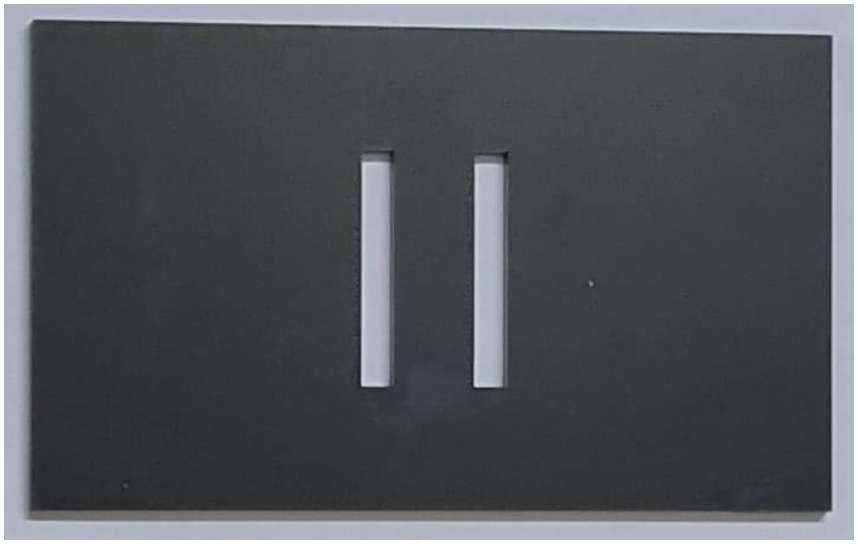

Figure 28: Acrylic Base Plate after Laser Cutting

Power System Design

A key step in the design, analysis, and fabrication of a quadruped robot is the set up of a sufficient and effective power system. For our quadruped, a series of tests were performed on the prototype leg for setting up a vigorous power system for the whole quadruped.

- Microcontroller

To control the servo motors of the quadruped, Arduino Mega 2560 has been used. The Arduino mega board has been protected using the sensor shield V1 to reduce the excess use of wires and prevent losses. Arduino Mega 2560 has 54 digital pins for input and outputs out of which 15 pins can be used for PWM signals, this is more than sufficient to control the eight servo motors of our quadruped. Moreover, the mega board has 16 analog inputs, 4 UARTs (hardware serial ports), a 16 MHz crystal oscillator, a USB connection, a power jack, an ISCP header and reset button.

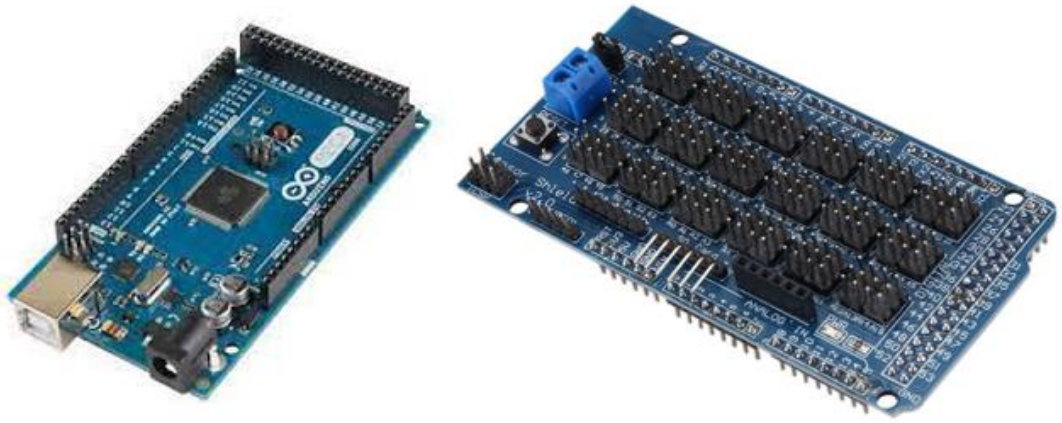

Figure 29: Arduino Mega 2560 and Sensor Shield

- Power Supply

It is worth mentioning the importance of selecting the appropriate and sufficient power supply has been chosen for smooth and safe functioning of the Arduino Mega board and the 8 servo actuators. The selection of the power supply has been done keeping the operating voltage and current ratings of the servos. In order to sufficiently power the eight servo motors, it was evident that we needed to incorporate a large power supply which can enable the servos to meet its high current requirement to operate under high torque and load. For this, we have decided to use Lithium-Ion Polymer rechargeable battery rated at 11.1V and 5200 mAh.

Figure 30: Rechargeable LiPo Battery as Power Supply

- Buck DC/DC Converter for Current Amplification

Running 8 servo motors simultaneously under high torque requires a significant amount of current boost and voltage. Such high-power requirement cannot be met by a single power supply alone and hence a DC-to-DC current amplification is achieved using a buck DC/DC converter. The buck converter is a basic DC-DC converter that provides an output voltage that is lower than the input voltage. The inductor in a buck converter always "bucks" or acts against the input voltage, hence the name. An ideal buck converter's output voltage is equal to the product of the switching duty cycle and the supply voltage.

The buck converter, like many other power supply topologies, works on the principle of storing energy in an inductor. Changes in electric current passing through an inductor cause a voltage drop across the device. The switching element, which is usually a power MOSFET or IGBT, should be either open or closed – off or on – so that the buck converter circuit may switch between two states.

Figure 31: Buck DC/DC Converter XL4016

For our requirement, we have incorporated XL4016 buck DC/DC converter having the following specifications.

Table 7: Buck DC/DC Specifications

Specifications	Details
Input Voltage Range	8V to 40V
Output Voltage Range	1.25V to 36V
Output Current Capacity	9A
Switching Frequency	180kHz Constant

Final Assembly of the Quadruped

The last step in the finalization of fabrication phase of our quadruped is the final assembly of the robot. The assembly has been done on the acrylic base plate, on which, all the eight servos of four legs, battery, microcontroller, and DC/DC converter have been mounted.

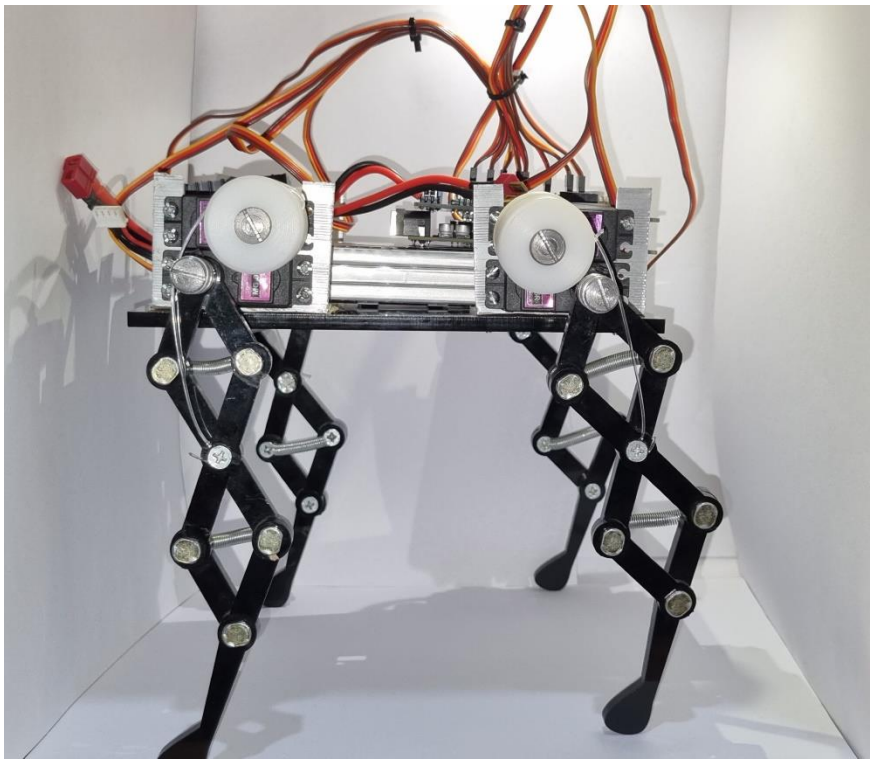

Figure 32: Final Assembly of the Quadruped (Side View)

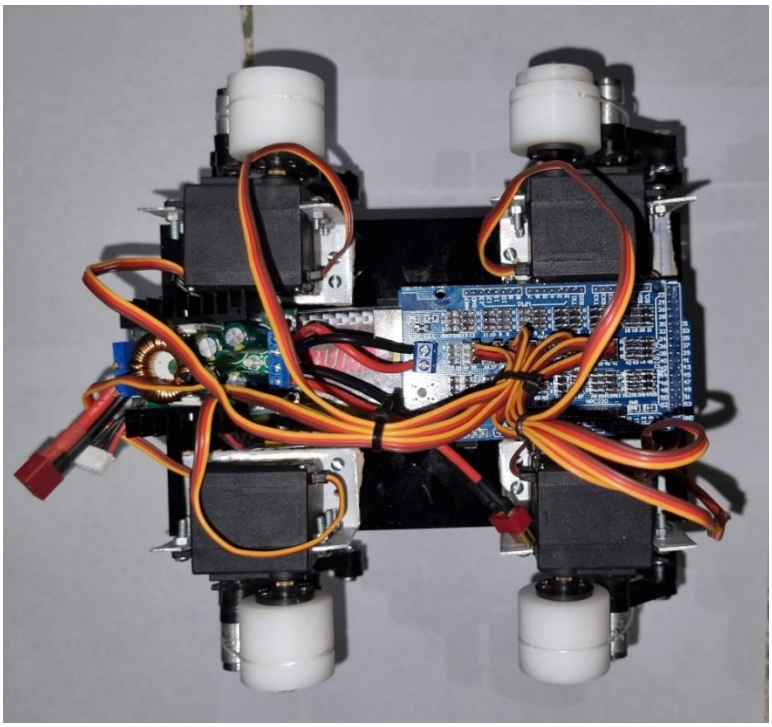

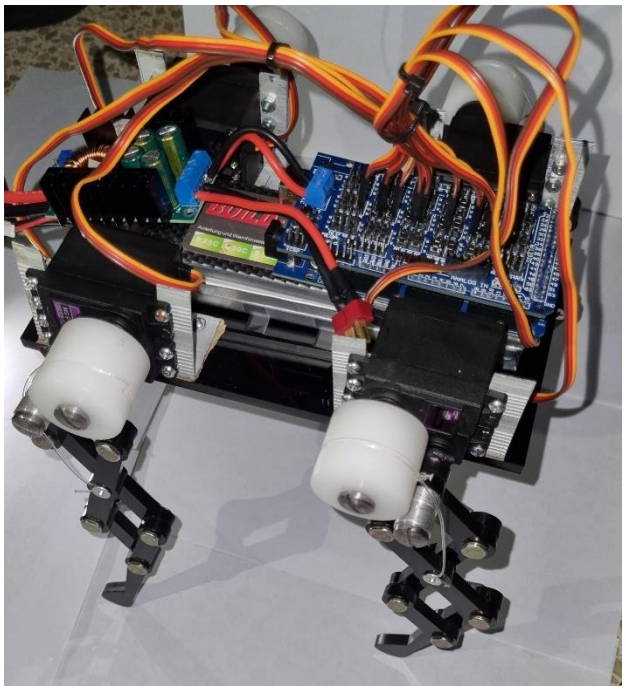

Figure 33: Final Assembly

CHAPTER 4: RESULTS AND DISCUSSIONS

Finite Element Model

FEM analysis has been incorporated during the design phase of the prototype leg. Basic model development of each link under different loadings and torques has been done to analyze the design safety of the parts.

FEM Analysis of the Leg Links

FEM analysis has been done on the leg links for the maximum force and torque which can occur on each link. A constant force of 80 N is estimated with a very high factor of safety, whereas a constant torque of 45 Nm is estimated on the pin joints. The value of torque is approximated from the stall torque of the servo motor MG 996R. As can be seen for the values of maximum Von Mises stresses and maximum deflection in the reports, none of the components fail even after such severe and unrealistic loads that were applied for a good factor of safety, which also accounts for impact loading.

- Base Links 1 and 2

The first two links in each leg are the two links directly connected to the servo motor via a pin joint. Following are the parameters used for stress analysis of this link.

Table 8: Model Parameters of Base Link 1 and 2

Model Parameters of Base Links 1 and 2	
Material	Acrylic
Fixtures	Pin Joint at both ends

Force Loadings	Constant force on the outer surface of 100 N
Torque Loadings	Torque at Pin Joints of 45 Nm

The following figures show the factor of safety plot for base links 1 and 2 under the discussed model.

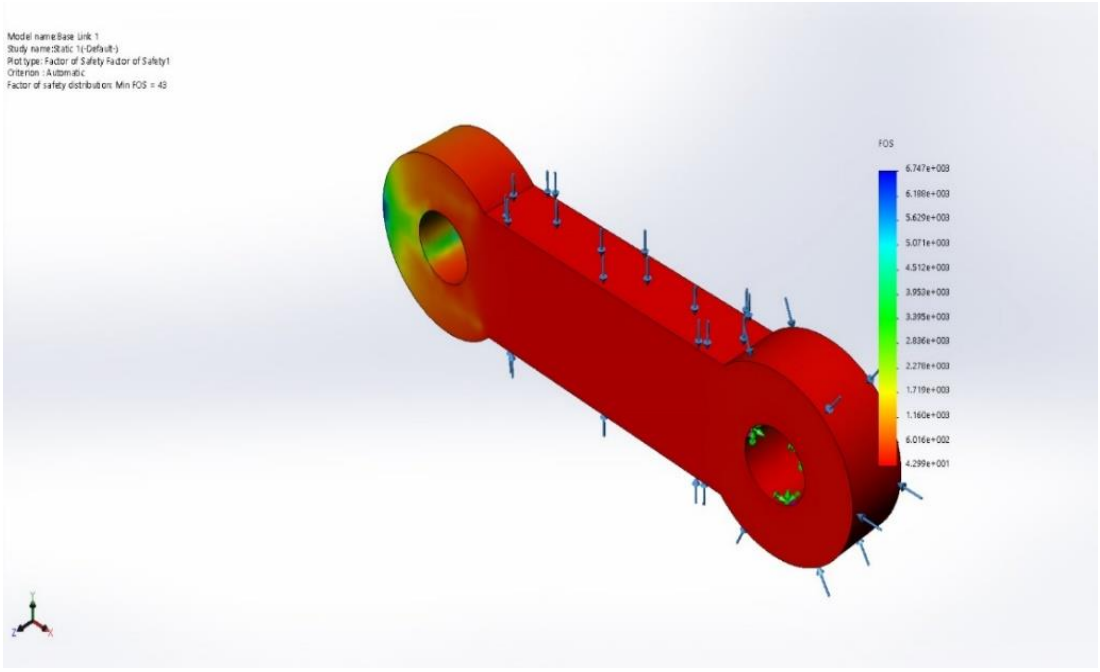

Figure 34: Base Link 1 Factor of Safety Plot

Figure 1 shows the factor of safety plot for the first base link. The FOS in the considered loading case and developed meshed model is found to be 43 i.e., a very high FOS indicates the safety of part.

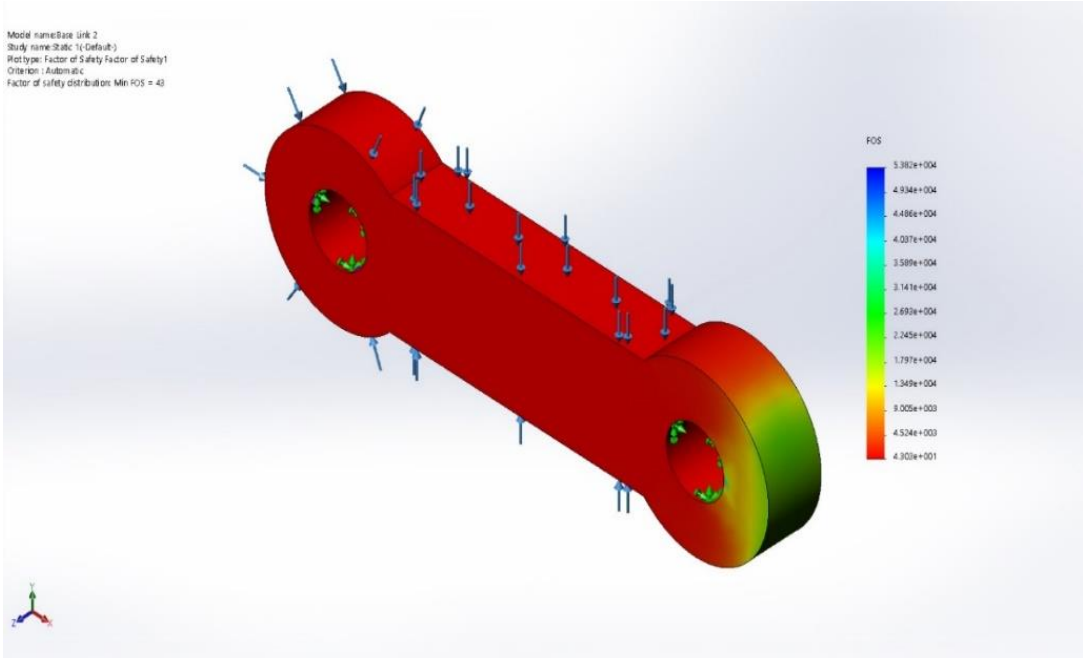

Figure 35: Base Link 2 Factor of Safety Plot

Similarly, figure 2 shows the factor of safety plot for the second base link. Since the loading condition is the same due to symmetry, hence the results obtained are identical. The FOS in the considered loading case and developed meshed model is found to be 43 i.e., a very high FOS indicates the safety of part.

Table 9: Extreme Loading Case Results for Base Links 1 and 2

Extreme Loading Case Results for Base Links 1 and 2	
Maximum Von Mises Stress	1.05 MPa
Maximum Displacement	2.7×10^{-3} mm

Detailed stress analysis and deformation results have been shown in Appendix I.

- Long Links 3 and 4

The two middle links are twice the length of the base links comprising of two end pins and a middle pin. The following parameters are set up for the stress analysis. Moreover, the middle pin joint has a connection to the second servo motor via a pulley.

Table 10: Model Parameters of Long Links 3 and 4

Model Parameters of Long Links 3 and 4	
Material	Acrylic
Fixtures	Pin Joint at both ends and in middle
Force Loadings	Constant force on the outer surface of 100 N
Torque Loadings	Torque at each pin connection of 45 Nm

The following figures show the factor of safety plots for the long links.

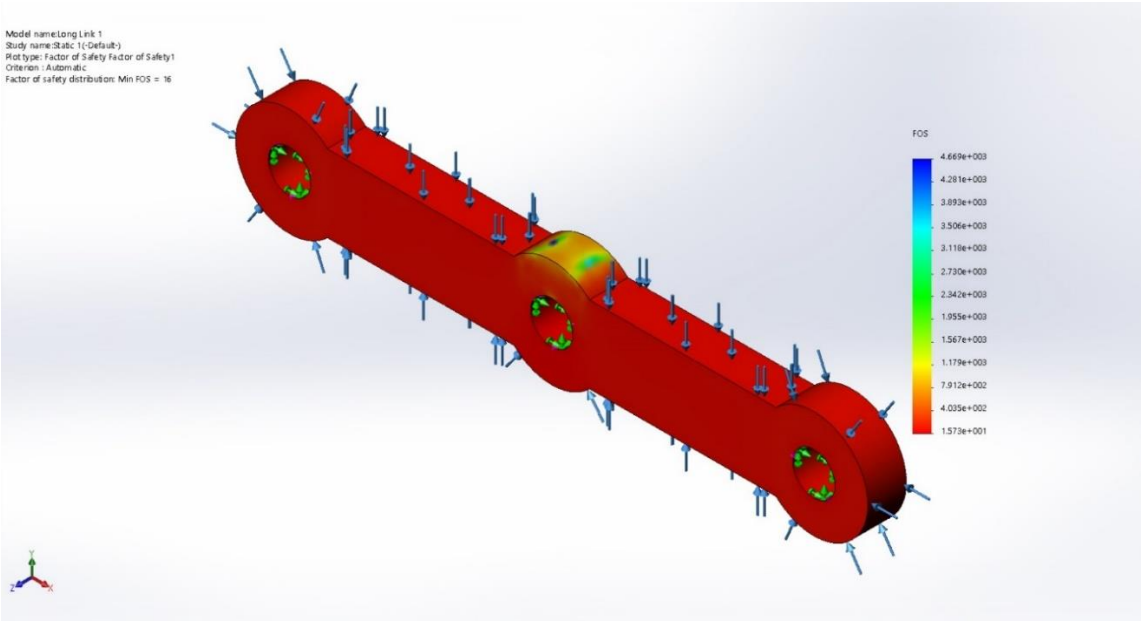

Figure 36: Factor of Safety Plot for Long Link 3 and 4

Figure 3 shows the factor of safety plot for Long Link 3 under extreme loading conditions. The computed minimum FOS is found to be 16, which is quite high and predicts the safety of the link in extreme loading conditions. The results will remain identical for both long links due to similar loading conditions.

Table 11: Extreme Loading Case Results for Long Links 3 and 4

Extreme Loading Case Results for Long Links 3 and 4	
Maximum Von Mises Stress	2.86 MPa
Maximum Displacement	2.9×10^{-3} mm

Detailed stress analysis and deformation results have been shown in Appendix I.

- Short Link 5

The short link is incorporated at the bottom to connect the last link with one of the long links. The link is not in direct connection with any of the two actuators, hence, there is not a direct application of torque or force. The following model is developed assuming the extreme loading conditions.

Table 12: Model Parameters for Shor Link 5

Model Parameters of Short Link 5	
Material	Acrylic
Fixtures	Pin Joint at both ends
Force Loadings	Constant force on the outer surface of 100 N

Torque Loadings	Torque at Pin Joints of 45 Nm

The following figure shows the factor of safety plot for link 5.

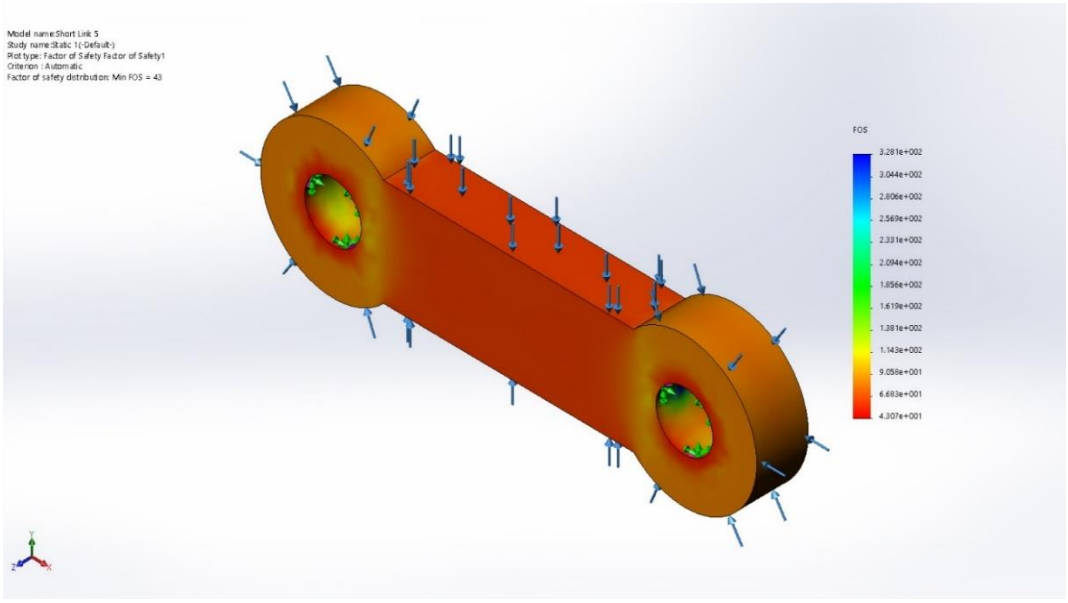

Figure 37: Factor of Safety Plot for Short Link 5

The factor of safety plot results in figure 4 indicates the minimum FOS of 42 i.e., under the extreme loading conditions. Similar to other links, link 5 also shows a very high FOS, predicting a safe application of the Acrylic part in the ELS quadruped leg.

Table 13: Extreme Loading Case Results for Short Link 5

Extreme Loading Case Results for Short Link 5	
Maximum Von Mises Stress	1.04 MPa
Maximum Displacement	1.27×10^{-3} mm

Detailed stress analysis and deformation results have been shown in Appendix I.

- Last Link 6

Finally, the last link i.e., link 6 of the quadruped leg has been considered. Similar to the other legs, a model for the last link has been developed assuming extreme loading conditions. The last link also comprises two pin joints, however, unlike the other links, the two pin joints are present at the upper edge and in the middle of the link.

Table 14: Model Parameters for Last Link 6

Model Parameters of Last Link	
Material	Acrylic
Fixtures	Pin Joint at the top end and in middle
Force Loadings	Constant force on the outer surface of 100 N
	A contact force of 5N at the bottom tip of the link
Torque Loadings	Torque at each pin connection of 45 Nm

A contact force loading condition is added to this link, which accounts for the contact point of the leg with the surface. The magnitude of the contact force is taken equal to the approximate weight of the quadruped.

$$Maximum\ Contact\ Force = Weight\ of\ the\ whole\ Quadruped$$

In the extreme case for one leg, the whole weight of the quadruped is maintained by only one leg. Hence, the contact force is estimated to be 20 N (i.e., 2 kg assumed total weight of the whole Quadruped).

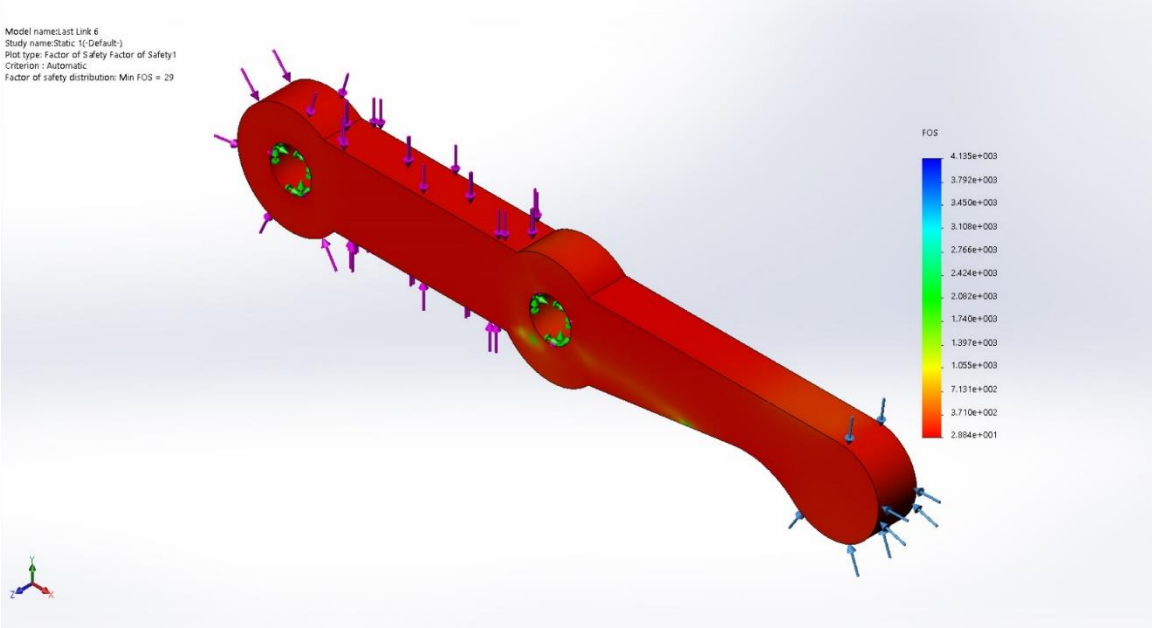

Figure 38: Factor of Safety Plot for Last Link

Figure 5 shows the factor of safety plot for the last link under extreme loading conditions. Similar to the other links, even in impractical and unrealistic loading cases, the acrylic-based link leg remains safe. The FOS predicted for the last link when under the weight of the whole quadruped is found to be 29, which is more than safe for our application.

Table 15: Extreme Loading Case Results for Last Link 6

Extreme Loading Case Results for Last Link	
Maximum Von Mises Stress	1.56 MPa
Maximum Displacement	3.55×10^{-3} mm

Detailed stress analysis and deformation results have been shown in Appendix I.

MATLAB Simulink Model of the Quadruped

To perform the detailed analysis on the design of the quadruped and study the mechanical aspect of the design, a Simulink model has been created using MATLAB. Firstly, a Simulink model for one leg of the quadruped is formed. Simulink attributes of 3D transformation has been incorporated to replicate the link transformations of the leg. Similarly, revolute joints have been used to model the link joints.

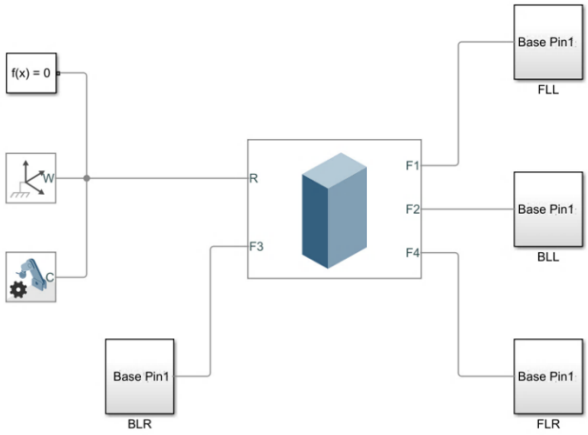

Figure 39: Simulink Model of the Quadruped

Following figure shows the 3D of the quadruped generated via Simulink.

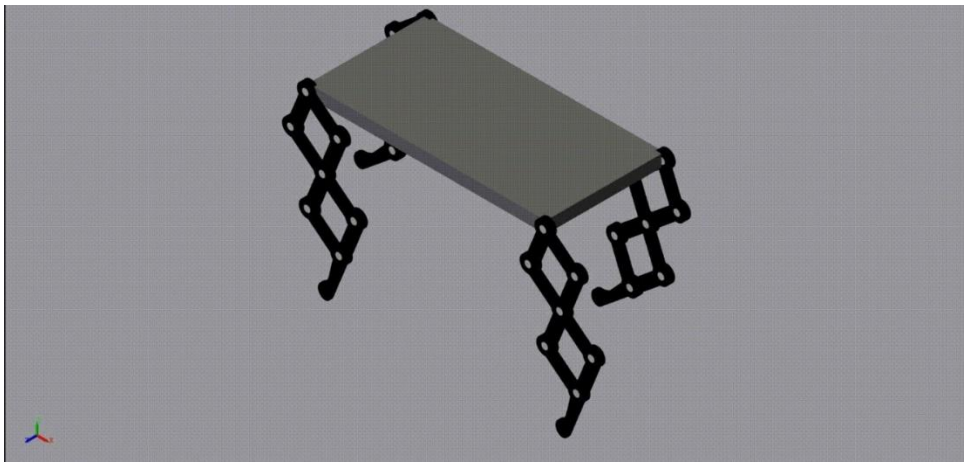

Figure 40: Simulink Model of the Quadruped

CHAPTER 5: CONCLUSION AND RECOMMENDATIONS

The team completed the mechanical design of the robot along with all associated calculations through a rigorous iterative process in order to achieve the goal of designing a hopping quadruped robot. The goal in essence was achieved using five bar planar mechanism.

For the purpose of finalizing a mechanical design of the quadruped robot, we went through various design by getting help from existing working models such as Super Mini Cheetah, Stanford Doggo, RHex, ANYmal and Ghost Minitaur.

The design was made to go through many possible improvements such as mass reduction, inertia reduction and different motors alternative until finalized. Structural analysis was performed in order to measure the effect of external forces on the robot and forces and stresses were calculated on the individual components of the robot. As a result, our design went through various design iterations in order to meet specific needs with respect to the overall weight, motor torques and cost constraints on the way to completion.

Our robot utilizes Elastic Scissor Mechanism (ELS) for the leg mechanism and motors are connected directly in order to reduce friction losses, delays due to transmission of motion not being direct and provide as much torque to the robot as possible without compensating the rotation speed of the revolute joints.

The quadruped has been modeled in Simulink and simulated the walking gait of quadrupedal, thus achieving the objective of stable locomotion simulation in the modified project scope. Actuator torques were calculated and plotted concluding that the chosen actuators and the design of the robot is adequate.

Recommendations for future work include implementing various gaits to test if the actuators are suitable for multiple gaits. A lot of simplification in design had to be done to make the actuators available in our budget to be usable. There are better actuators and better motor controllers available which can grant a huge amount of freedom in terms of

design and having complex mechanisms in the robot to achieve heavy-duty tasks instead of just walking in a straight line. The robot designed in this paper can only walk in a straight line since it is an 8 Degree-of-Freedom robot. Further work could involve adding 4 more actuators, one at each leg, to make the robot a 12 Degree-of-Freedom robot so that it can turn and walk on curved paths. The 5-bar mechanism for the legs was chosen to reduce weight but it is not a depiction of actual quadrupedal limbs. The design can be modified to include springs to make the mechanism compliant and more closely represent limbs of a quadrupedal. The Spring-loaded Pantograph or the Advanced Spring-loaded Pantograph designs are better for this purpose. All that is needed are stronger and more reliable actuators and their corresponding motor controllers. Another recommendation would be to incorporate machine learning into the robot. Spatial awareness and obstacle detection can be introduced. Sensors can be incorporated, and a complex closed-loop control system can be designed so that the robot can detect obstacles and avoid them. Extensions such as robotic arms can be integrated with quadrupeds to perform various takes. This idea is similar to Boston Dynamic's Spot mini.

These are the recommendations that we have proposed that will help to improve this project and develop it further.

REFERENCES

[1] I. R. Nourbakhsh, D. Scaramuzza, and R. Seigwart, *Introduction to Autonomous Mobile Robots*, 2nd ed. MIT Press, 2011.

[2] J. C. Larsen and K. Stoy, "Energy Efficiency of Robot Locomotion Increases Proportional to Weight [Extended Abstract]."

[3] N. Kau, A. Schultz, N. Ferrante, and P. Slade, "Stanford Doggo : An Open-Source , Quasi-Direct-Drive Quadruped," pp. 6309–6315, 2019.

[4] W. Bosworth, S. Kim, and N. Hogan, "The MIT Super Mini Cheetah : A small , low-cost quadrupedal robot for dynamic locomotion," *2015 IEEE Int. Symp. Safety,*

Secur. Rescue Robot., pp. 1–8.

[5] G. Kenneally and D. E. Koditschek, “Design Principles for a Family of Direct-Drive Legged Robots Design Principles for a Family of Direct-Drive Legged Robots,” vol. 1, no. 2, pp. 900–907, 2016.

[6] Q. Sun, C. Wang, D. Zhao, and C. Zhang, “Cam Drive Step Mechanism of a Quadruped Robot,” vol. 2014, 2014.

[7] M. H. Raibert *et al.*, “Stable Locomotion,” no. 4148, 1983.

[8] S. Cotton, I. M. C. Olaru, M. Bellman, T. Van Der Ven, J. Godowski, and J. Pratt, “FastRunner: A fast, efficient and robust bipedal robot. Concept and planar simulation,” *Proc. - IEEE Int. Conf. Robot. Autom.*, pp. 2358–2364, 2012.

[9] N. Moore and M. Buehler, “RHex : A Biologically Inspired Hexapod Runner ∗,” pp. 207–213, 2001.

[10] R. J. Full and D. E. Koditschek, “Templates and anchors: neuromechanical hypotheses of legged locomotion on land,” *J. Exp. Biol.*, vol. 2, no. 12, pp. 3–125, 1999.

[11] J. Laumond, M. Benallegue, J. Carpentier, and A. Berthoz, “The Yoyo-Man HAL Id : hal-01175591,” no. September, 2015.

[12] R. M. Ghigliazza, R. Altendorfer, P. Holmes, D. E. Koditschek, R. Altendorfer, and P. Holmes, “A Simply Stabilized Running Model,” *Repr. from SIAM J. Appl. Dyn. Syst.*, vol. 2, no. 2, pp. 187–218, 2004.

[13] S. Kim and P. M. Wensing, “Design of Dynamic Legged Robots,” *Found. Trends Robot.*, vol. 5, no. 2, pp. 117–190, 2017.

[14] R. M. N. Alexander, “Three Uses For Springs in Legged Locmotion,” *Int. J. Rob. Res.*, vol. 9, no. 2, pp. 53–61, 1990.

[15] R. M. N. Alexander, M. B. Bennett, and R. F. Ker, “Mechanical Properites and Function of the Paw Pads of Some Mammals,” *J. Zool.*, pp. 405–419, 1986.

[16] R. M. Alexander, “Elastic energy stores in running vertebrates,” *Integr. Comp. Biol.*, vol. 24, no. 1, pp. 85–94, 1984.

[17] M. Hutter, “StarlETH & Co. – Design and control of legged robots with compliant actuation,” ETH Zurich, 2003.

[18] S. Arumugom, S. Muthuraman, and V. Ponselvan, “Modeling and Application of Series Elastic Actuators for Force Control Multi Legged Robots,” vol. 1, no. 1, pp. 26–33, 2009.

[19] A. Spröwitz, A. Tuleu, M. Vespignani, M. Ajallooeian, E. Badri, and A. J. Ijspeert, “Towards dynamic trot gait locomotion : Design , control , and experiments with Cheetah-cub , a compliant quadruped,” vol. 215, 2013.

[20] R. Altendorfer, N. Moore, H. Komsuo, M. Buehler, and D. E. Koditschek, “RHex : A Biologically Inspired Hexapod Runner 1,” 2000.

[21] D. J. Blackman, J. V Nicholson, C. Ordonez, B. D. Miller, and E. Jonathan, “Gait Development On Minitaur , A Direct Drive Quadrupedal Robot,” vol. 9837, pp. 1–15, 2016.

[22] M. Hutter *et al.*, “ANYmal - A Highly Mobile and Dynamic Quadrupedal Robot *,” *2016 IEEE/RSJ Int. Conf. Intell. Robot. Syst.*, pp. 38–44, 2016.

[23] “7 THINGS TO CONSIDER WHEN CHOOSING AN ALUMINUM GRADE,” 2015. .

[24] J. W. Hurst, “The Electric Cable Differential Leg: A Novel Design Approach for Walking and Running,” 2010.

[25] H. Witte, R. Hackert, W. Ilg, J. Biltzinger, N. Schilling, F. Biedermann, M. Jergas, H. Preuschoft, and M. Fischer, ``Quadrupedal mammals as paragons for walking machines," in Proc. Int. Symp. Adapt. Motion Ani-mals Mach. (AMAM), Montreal, QC, Canada, 2000, pp. 1-6.

[26] A. Spröwitz, A. Tuleu, M. Vespignani, M. Ajallooeian, E. Badri, and A. J. Ijspeert, ``Towards dynamic trot gait locomotion: Design, control, and experiments with cheetah-cub, a compliant quadruped robot," Int. J. Robot. Res., vol. 32, no. 8, pp. 932950, Jul. 2013.

[27] A. T. Spröwitz, A. Tuleu, M. Ajallooeian, M. Vespignani, R. Möckel, P. Eckert, M. D'Haene, J. Degrave, A. Nordmann, B. Schrauwen, J. Steil, and A. J. Ijspeert, ``Oncilla robot: A versatile open-source quadruped research robot with compliant pantograph legs," Frontiers Robot. AI, vol. 5, p. 67, Jun. 2018.

[28] S. Rutishauser, A. Sprowitz, L. Righetti, and A. J. Ijspeert, ``Passive compliant quadruped robot using central pattern generators for locomotion control," in Proc. 2nd IEEE RAS EMBS Int. Conf. Biomed. Robot. Biomechtron., Oct. 2008, pp. 710715.

[29] M. H. A. Nizami et al., "Proximal Actuation of an Elastically Loaded Scissors Mechanism for the Leg Design of a Quadruped Robot," in IEEE Access, vol. 8, pp. 208240-208252, 2020, doi: 10.1109/ACCESS.2020.3037250.

APPENDIX I: SIMULATION FEM REPORT

The simulation results are displayed below. For each component, the first profile is the von Mises stresses and the second profile is the deflection.

Base Link 1

Name	Type	Min	Max
Stress1	VON: von Mises Stress	6.670e+003N/m^2 Node: 216	1.047e+006N/m^2 Node: 9801

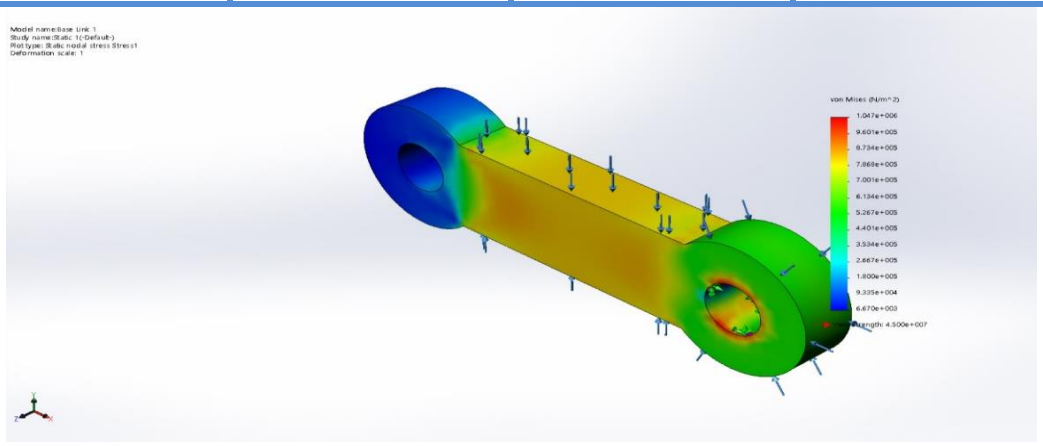

Base Link 1-Static 1-Stress-Stress1

Name	Type	Min	Max
Displacement1	URES: Resultant Displacement	0.000e+000mm Node: 1	2.723e-003mm Node: 11372

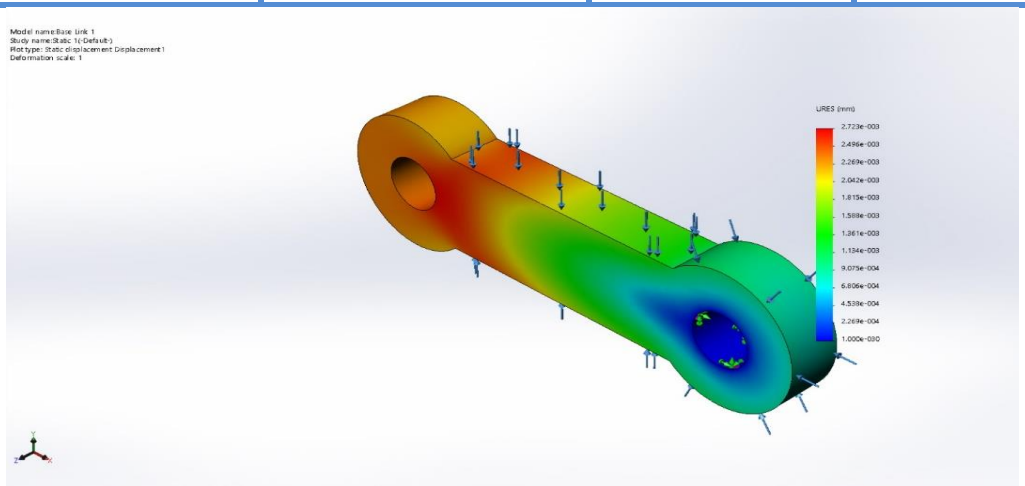

Base Link 1-Static 1-Displacement-Displacement1

Base Link 2

Name	Type	Min	Max
Stress1	VON: von Mises Stress	8.362e+002N/m^2 Node: 43	1.046e+006N/m^2 Node: 11638

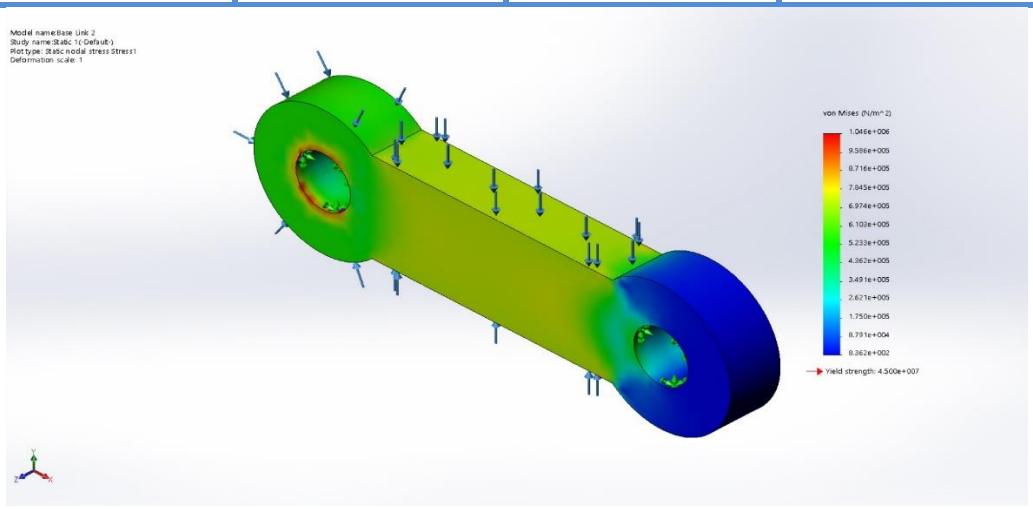

Base Link 2-Static 1-Stress-Stress1

Name	Type	Min	Max
Displacement1	URES: Resultant Displacement	0.000e+000mm Node: 1	1.298e-003mm Node: 321

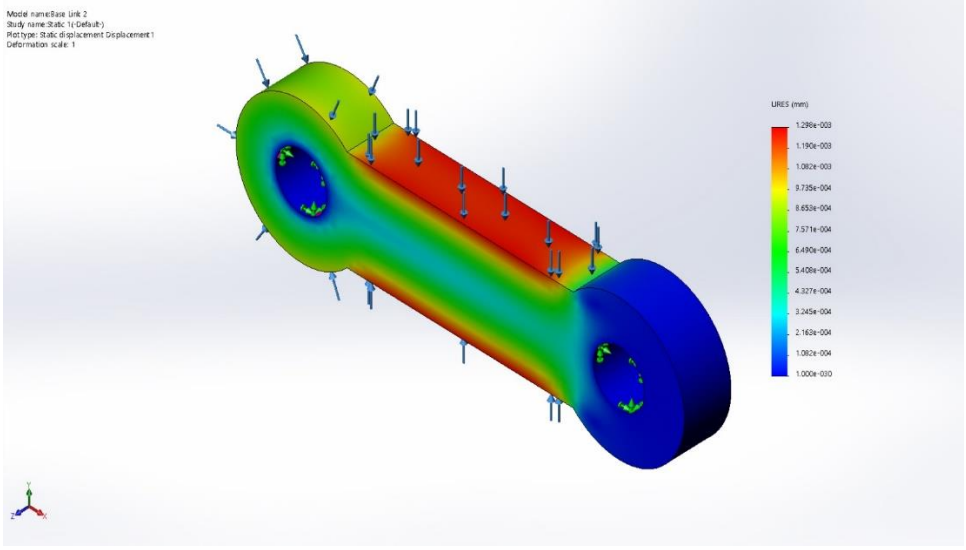

Base Link 2-Static 1-Displacement-Displacement1

Long Links 3 and 4

Name	Type	Min	Max
Stress1	VON: von Mises Stress	9.638e+003N/m^2 Node: 5688	2.861e+006N/m^2 Node: 55

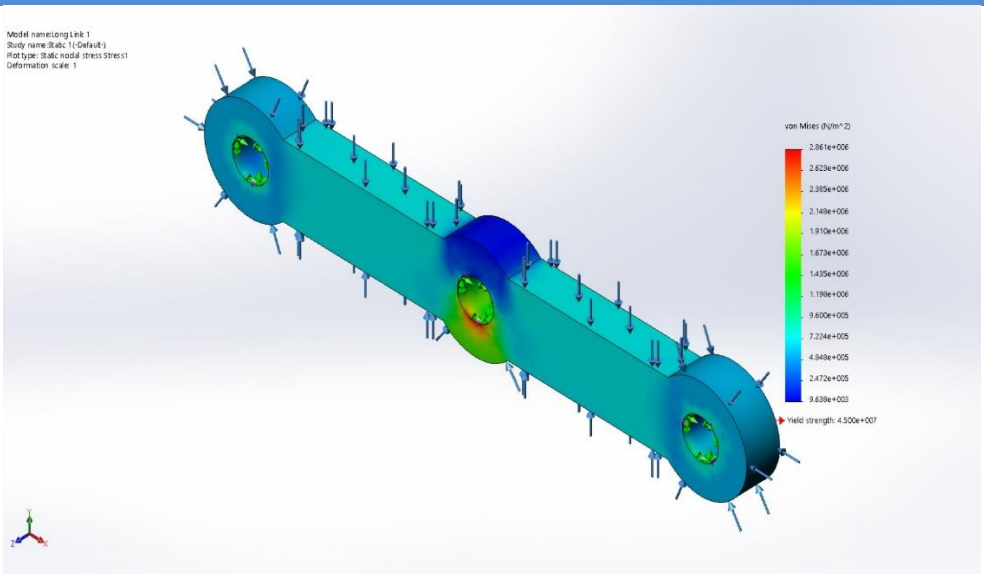

Long Link 1-Static 1-Stress-Stress1

Name	Type	Min	Max
Displacement1	URES: Resultant Displacement	0.000e+000mm Node: 1	2.916e-003mm Node: 8463

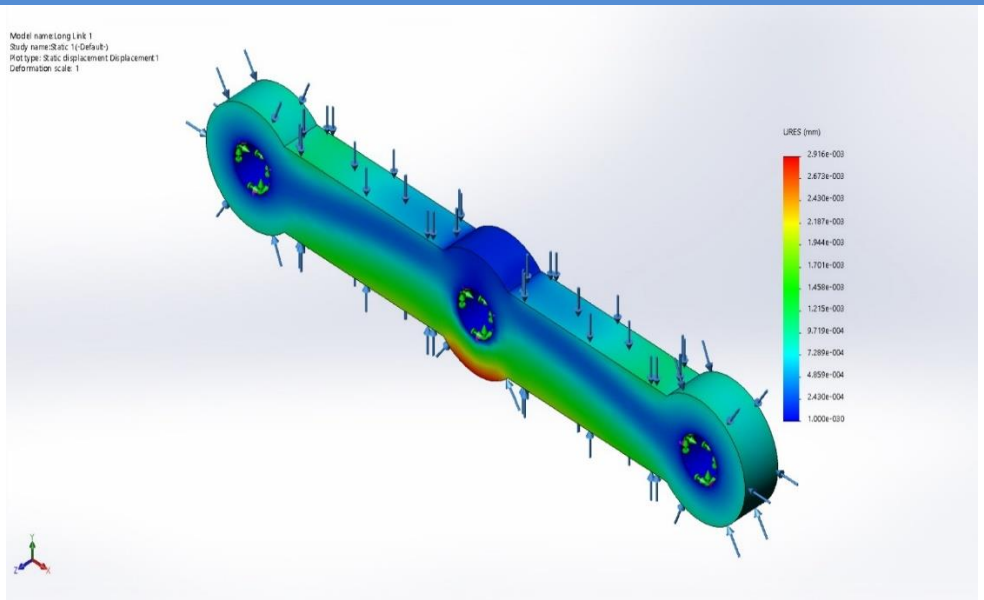

Long Link 1-Static 1-Displacement-Displacement1

Short Link 5

Name	Type	Min	Max
Stress1	VON: von Mises Stress	1.371e+005N/m^2 Node: 17	1.045e+006N/m^2 Node: 11638

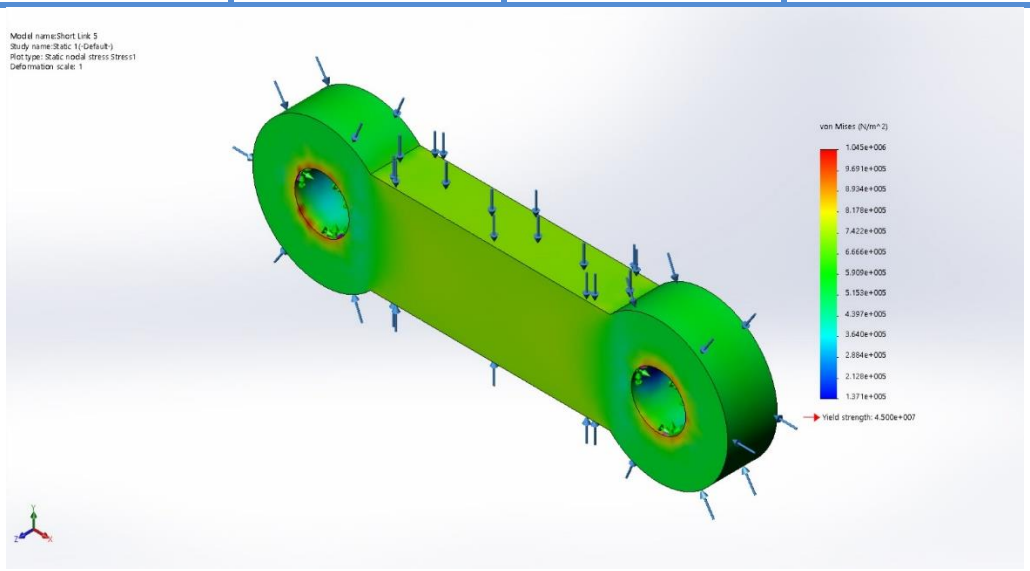

Short Link 5-Static 1-Stress-Stress1

Name	Type	Min	Max
Displacement1	URES: Resultant Displacement	0.000e+000mm Node: 1	1.272e-003mm Node: 8056

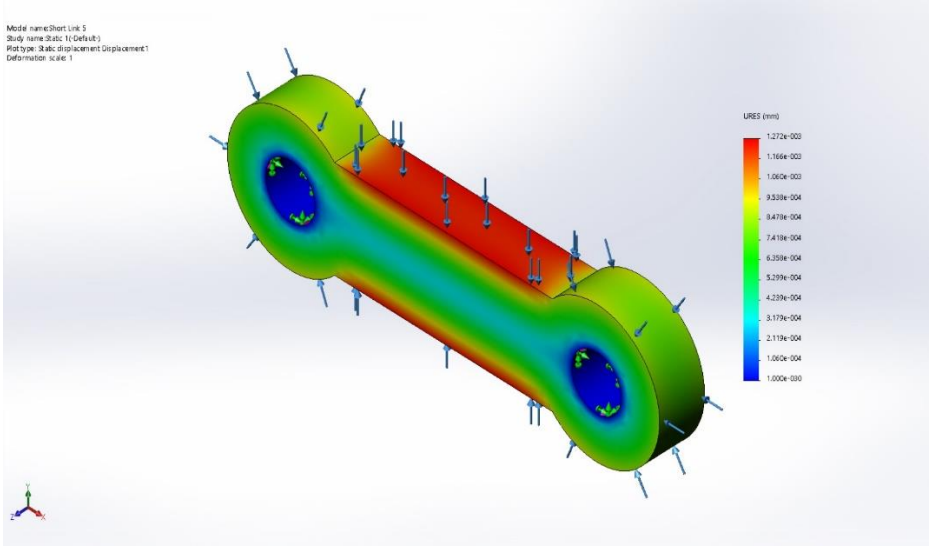

Short Link 5-Static 1-Displacement-Displacement1

Last Link 6

Name	Type	Min	Max
Stress1	VON: von Mises Stress	1.088e+004N/m^2 Node: 10204	1.560e+006N/m^2 Node: 8257

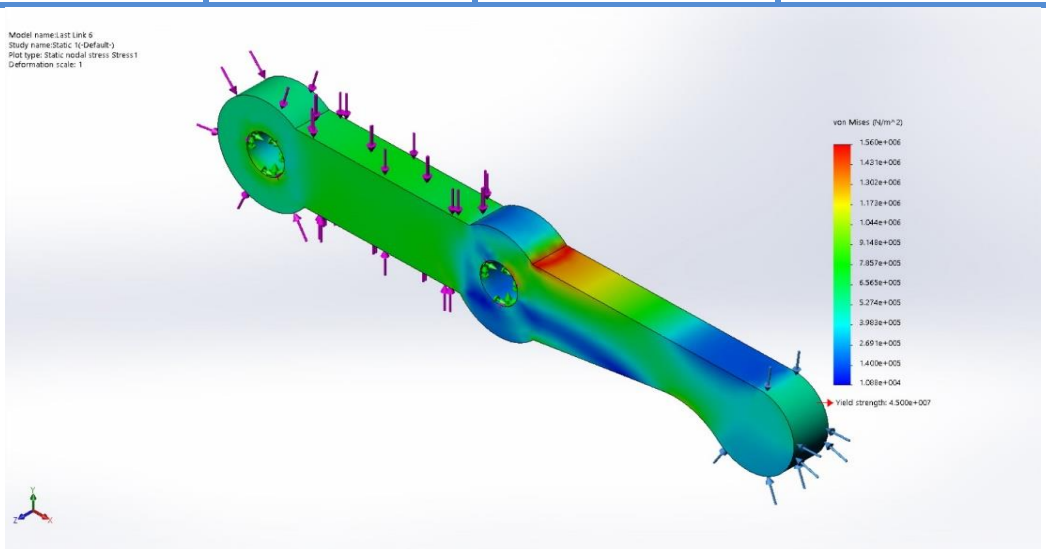

Last Link 6-Static 1-Stress-Stress1

Name	Type	Min	Max
Displacement1	URES: Resultant Displacement	0.000e+000mm Node: 1	3.541e-002mm Node: 10983

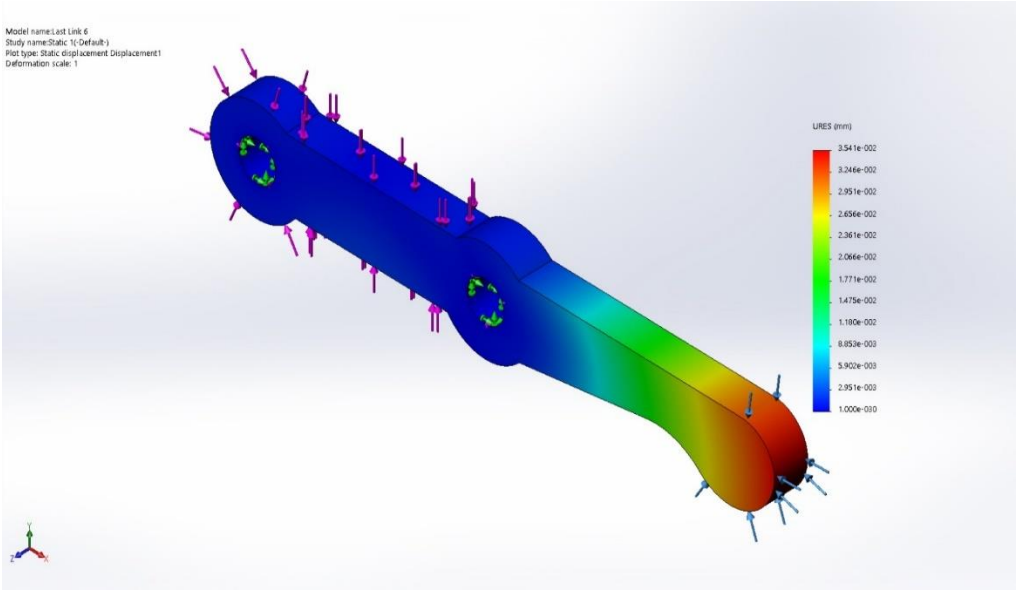

Last Link 6-Static 1-Displacement-Displacement1

APPENDIX II: MATLAB CODES AND CALCULATIONS

MATLAB Code for Forward Kinematics of the Leg

```
syms L thet1 thet2 thet3 thet4 thet5 thet6 bx by bz;
alp= [0 180 180 180 180 180];
a = [0 0 L 0 2*L 0];
d = [0 0 0 0 0 0];
theta = [thet1 180-2*thet1 thet3 thet3 thet5 thet6];

for i = 1:6
   T = [cosd(theta(i)) -sind(theta(i)) 0 a(i);
      cosd(alp(i))*sind(theta(i)) cosd(alp(i))*cosd(theta(i)) -sind(alp(i)) -d(i)*sind(alp(i));
      sind(alp(i))*sind(theta(i)) sind(alp(i))*cosd(theta(i)) cosd(alp(i)) d(i)*cosd(alp(i));
      0 0 0 1];
   if i == 1
      T0_1 = T
   end
   if i == 2
      T1_2 = T
   end
   if i == 3
      T2_3 = T
   end
   if i == 4
      T3_4 = T
   end
   if i == 5
      T4_5 = T
   end
  if i ==6
     T5_6 = T
  end
end


T0_6 = T0_1*T1_2*T2_3*T3_4*T4_5*T5_6

% base frame coordinates (assume)
Base_Frame_Cord = [bx; by; bz; 1]

% end effector cordinates
End_Effector_Cord = T0_6 * Base_Frame_Cord
```

Calculations for Inverse Kinematics of the Leg

We used symmetry to simplify the 6-DOF leg to a 3-DOF linkage.

The y-coordinate of the leg can be determined as follows:

$$y = l\cos\left(\varphi_1 - \frac{\pi}{2}\right) + 2l\sin\left(\frac{\varphi_2}{2}\right) + 2l\sin\left(\frac{\varphi_2}{2}\right)$$

$$\rightarrow y = l\sin(\varphi_1) + 4l\sin\left(\frac{\varphi_2}{2}\right)$$

The x-coordinate of the leg can be determined in 2 ways:

$$x = l\,sin\left(\varphi_1 - \frac{\pi}{2}\right) + 2l\cos\left(\frac{\varphi_2}{2}\right) - 2l\cos\left(\frac{\varphi_2}{2}\right)$$

$$\rightarrow x = -l\cos(\varphi_1)$$

OR

$$x = l\cos\left(\frac{\varphi_2}{2}\right) + 2l\cos\left(\frac{\varphi_2}{2}\right) - 2l\cos\left(\frac{\varphi_2}{2}\right)$$

$$\rightarrow x = l\cos\left(\frac{\varphi_2}{2}\right)$$

$$y = l\sin(\varphi_1) + 4l\sin\left(\frac{\varphi_2}{2}\right)$$

$$x = -l\cos(\varphi_1) = l\cos\left(\frac{\varphi_2}{2}\right)$$

We now determine R as follows:

$$R^2 = (-l\cos(\varphi_1))^2 + \left(l\sin(\varphi_1) + 4l\sin\left(\frac{\varphi_2}{2}\right)\right)^2$$

$$R^2 = l^2\cos^2(\varphi_1) + l^2\sin^2(\varphi_1) + 16l^2\sin^2\left(\frac{\varphi_2}{2}\right) + 8l^2\sin(\varphi_1)\sin\left(\frac{\varphi_2}{2}\right)$$

$$R^2 = l^2 + 8l^2 - 8l^2\cos(\varphi_2) + 8l^2\sin(\varphi_1)\sin\left(\frac{\varphi_2}{2}\right)$$

$$R^2 = 9l^2 - 8l^2\cos(\varphi_2) + 8l^2\sin\left(\pi - \frac{\varphi_2}{2}\right)\sin\left(\frac{\varphi_2}{2}\right)$$

$$R^2 = 9l^2 - 8l^2\cos(\varphi_2) + 8l^2\cos\left(\frac{\varphi_2}{2}\right)\sin\left(\frac{\varphi_2}{2}\right)$$

$$R^2 = 9l^2 - 8l^2\cos(\varphi_2) + 4l^2\sin(\varphi_2)$$

$$y = l\sin(\varphi_1) + 4l\sin\left(\frac{\varphi_2}{2}\right)$$

$$x = -l\cos(\varphi_1) = l\cos\left(\frac{\varphi_2}{2}\right)$$

We now solve for φ_2 as follows,

$$\boldsymbol{\varphi_2 = 2\,cos^{-1}\left(\frac{x}{l}\right)}$$

We now solve for φ_1 as follows,

$$y = l\sin(\varphi_1) + 4l\sin\left(\frac{\varphi_2}{2}\right)$$

Knowing that,

$$cos\left(\frac{\varphi_2}{2}\right) = \frac{x}{l}$$

And with basic knowledge of trigonometric ratios and Pythagorean theorem, we can determine:

$$\sin\left(\frac{\varphi_2}{2}\right) = \left(\frac{\sqrt{l^2 - x^2}}{l}\right)$$

$$y = l\sin(\varphi_1) + 4l\sin\left(\frac{\varphi_2}{2}\right)$$

$$x = -l\cos(\varphi_1) = l\cos\left(\frac{\varphi_2}{2}\right)$$

$$\varphi_2 = 2\cos^{-1}\left(\frac{x}{l}\right)$$

Hence,

$$y = l\sin(\varphi_1) + 4l \times \frac{\sqrt{l^2 - x^2}}{l}$$

$$\rightarrow y = l\sin(\varphi_1) + 4l\sqrt{\frac{l^2 - x^2}{l^2}}$$

$$\rightarrow \sin(\varphi_1) = \frac{y - 4l\sqrt{\frac{l^2 - x^2}{l^2}}}{l}$$

$$\rightarrow \boldsymbol{\varphi_1 = \sin^{-1}\left(\frac{y - 4l\sqrt{\frac{l^2 - x^2}{l^2}}}{l}\right)}$$

MATLAB Code for Inverse Kinematics of the Leg

Alternatively, MATLAB can be used to solve the following system of equations:

$$y = l\sin(\varphi_1) + 4l\sin\left(\frac{\varphi_2}{2}\right)$$

$$x = -l\cos(\varphi_1) = l\cos\left(\frac{\varphi_2}{2}\right)$$

```
syms x y phi1 phi2 L
Result = solve(x==L*cos(phi2/2), y == L*sin(phi1) + 4*L*sin(phi2/2), phi1, phi2)
phi1 = Result.phi1(4)
phi2 = Result.phi2(2)
```

APPENDIX III: MATLAB SIMULINK MODEL

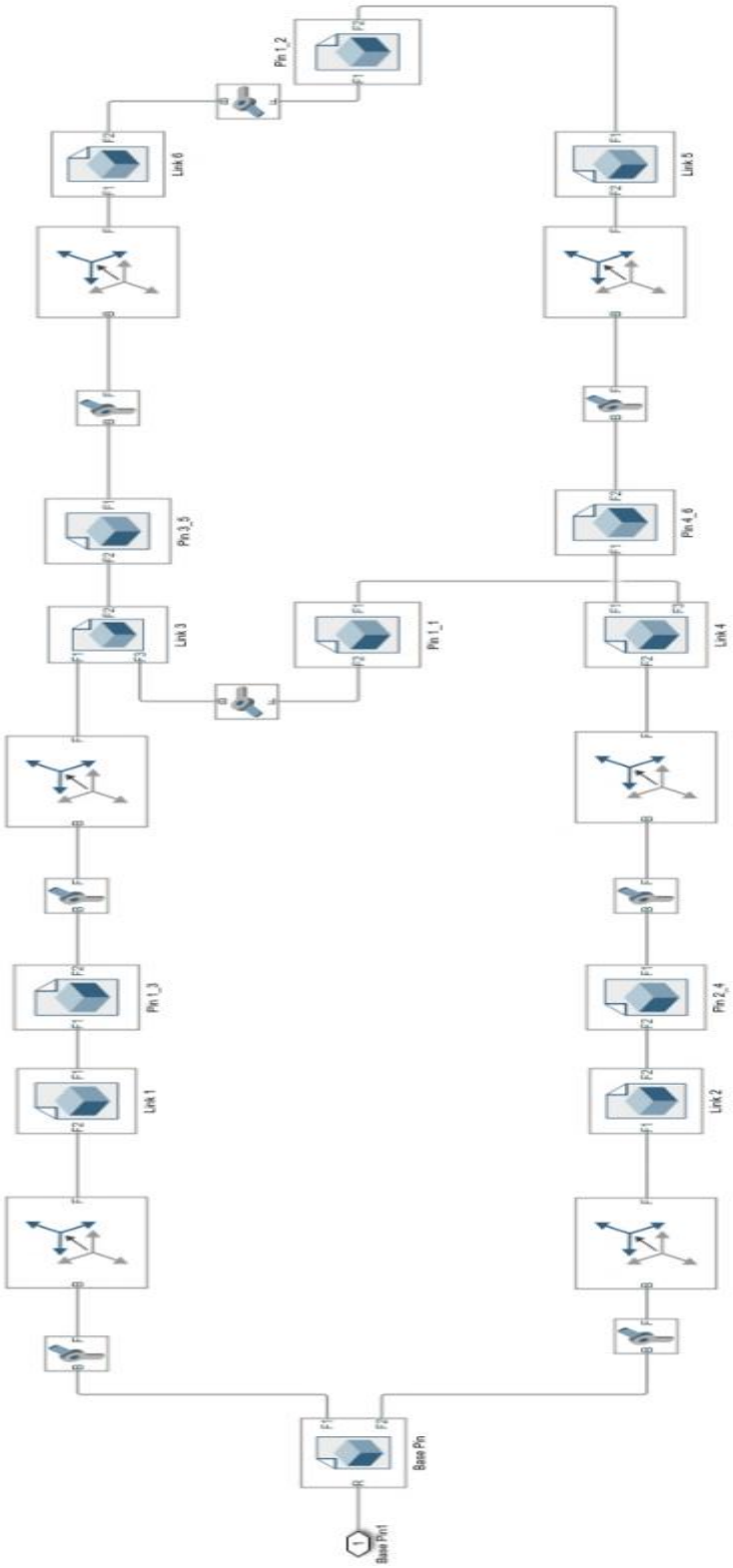

APPENDIX IV: CONTROL SYSTEM ARDUINO CODE

```
// this library is imported from github
// it allows for unique functions to be used for a more optimized control
system
#include "YouMakeRobots.h"

YouMakeRobots robot;

/*
  The motors are connected as such:
      Right Front Leg Swing   Motor  -  0   (pin 22)
      Right Rear  Leg Swing   Motor  -  1   (pin 23)
      Left  Front Leg Swing   Motor  -  2   (pin 24)
      Left  Rear  Leg Swing   Motor  -  3   (pin 25)
      Right Front Leg Retract Motor  -  4   (pin 26)
      Right Rear  Leg Retract Motor  -  5   (pin 27)
      Left  Front Leg Retract Motor  -  6   (pin 28)
      Left  Rear  Leg Retract Motor  -  7   (pin 29)
*/

void setup() {
  Serial.begin(115200);

  robot.init();
  robot.initialPosition();
  robot.executeCommand("TRIM:0=40,1=40,2=40,3=40");
  walk(5);
}

void loop() {
  // This function is skipped as we need the loop to stop after 5 steps
}

void serialEvent() {
  // this function sends commands to the serial monitor
  String cmd;
  cmd=Serial.readString();
  robot.executeCommand(cmd);
}
```

```
void walk(unsigned int n) {
  // a new function is created to make the quadruped walk n steps
  for(unsigned int i=0;i<n;i++) {

    //home position
    robot.executeCommand("MOVE:0=0,1=0,2=0,3=0,4=0,5=0,6=0,7=0");
    //front right and rear left legs retract and extend forward
    robot.executeCommand("MOVE:0=20,3=20,4=50,7=50");
    //front right and rear left legs return to home position while the fro
nt left and rear right retract and extend forward
    robot.executeCommand("MOVE:0=0,1=20,2=20,3=0,4=0,5=50,6=50,7=0");
    //front left and rear right return to home position
    robot.executeCommand("MOVE:1=0,2=0,5=0,6=0");
  }
}
```